Mehmet Furkan Baltacıoğlu DESIGN OF LIGHTWEIGHT AND COMPACT KNEE-ANKLE ASSISTIVE DEVICE FOR WALKING AND SIT TO STANCE AGU 2018

DESIGN OF LIGHTWEIGHT AND COMPACT KNEE-ANKLE ASSISTIVE DEVICE FOR WALKING AND SIT TO STANCE

A THESIS
SUBMITTED TO THE DEPARTMENT OF ADVANCED MATERIALS AND NANOTECHNOLOGY
AND THE GRADUATE SCHOOL OF ENGINEERING AND SCIENCE OF ABDULLAH GUL UNIVERSITY
IN PARTIAL FULFILLMENT OF THE REQUIREMENTS
FOR THE DEGREE OF MASTER OF SCIENCE

By
Mehmet Furkan Baltacıoğlu
December 2018

DESIGN OF LIGHTWEIGHT AND COMPACT KNEE-ANKLE ASSISTIVE DEVICE FOR WALKING AND SIT TO STANCE

A THESIS
SUBMITTED TO THE DEPARTMENT OF ADVANCED MATERIALS AND NANOTECHNOLOGY
AND THE GRADUATE SCHOOL OF ENGINEERING AND SCIENCE OF ABDULLAH GUL UNIVERSITY
IN PARTIAL FULFILLMENT OF THE REQUIREMENTS
FOR THE DEGREE OF MASTER OF SCIENCE

By
Mehmet Furkan Baltacıoğlu
December 2018

SCIENTIFIC ETHICS COMPLIANCE

I hereby declare that all information in this document has been obtained in accordance with academic rules and ethical conduct. I also declare that, as required by these rules and conduct, I have fully cited and referenced all materials and results that are not original to this work.

Mehmet Furkan BALTACIOĞLU

REGULATORY COMPLIANCE

M.Sc thesis titled **"DESIGN OF LIGHTWEIGHT AND COMPACT KNEE-ANKLE ASSISTIVE DEVICE FOR WALKING AND SIT TO STANCE"** has been prepared in accordance with the Thesis Writing Guidelines of the Abdullah Gül University, Graduate School of Engineering & Science.

Prepared By	Advisor
Mehmet Furkan BALTACIOĞLU	Assistant Prof. Ramazan ÜNAL

Head of the Advanced Materials And Nanotechnology Program

Prof. Dr. Murat DURANDURDU

ACCEPTANCE AND APPROVAL

M.Sc thesis titled **"DESIGN OF LIGHTWEIGHT AND COMPACT KNEE-ANKLE ASSISTIVE DEVICE FOR WALKING AND SIT TO STANCE"** and prepared by Mehmet Furkan Baltacıoğlu has been accepted by the jury in the Advanced Materials and Nanotechnology Graduate Program at Abdullah Gül University, Graduate School of Engineering & Science.

20 / 12 / 2018

JURY:

Assistant Professor Ramazan ÜNAL:…….

Assistant Professor Burak BAL :…….

Associated Professor Recep EKİCİ :…….

APPROVAL:

The acceptance of this M.Sc. thesis has been approved by the decision of the Abdullah Gül University, Graduate School of Engineering & Science, Executive Board dated ….. /….. / …….. and numbered ……..……. .

…….. /…….. / ……..
Graduate School Dean
Prof. Dr. İrfan ALAN

ABSTRACT

DESIGN OF LIGHTWEIGHT AND COMPACT KNEE-ANKLE ASSISTIVE DEVICE FOR WALKING AND SIT TO STANCE

Mehmet Furkan Baltacıoğlu

Msc. in Advanced Materials and Nanotechnology

Superviser: Assistant Professor Ramazan Ünal

December 2018

In this study, design of a conceptual semi-active transfemoral prothesis which can be used for walking, sit-to-stand and stair climbing was studied. In this study, human data in literature were analyzed and according to these data, firstly conceptual design of the prosthesis was presented. The first initial concept design was also built by means of 3D printer. Thereafter according to built model, the conceptual design was modified to make it more stable for functions. Also, the theoretical spring coefficients were calculated. According to structural parameters, FEM analyses of prosthesis were made. And parts on prosthesis were optimized by using topology optimization process.

Keywords: Assistive Device, Design, Knee-Ankle, Human Gait

ÖZET

OTURUP KALKMA VE YÜRÜME İÇİN HAFİF AĞIRLIKLI VE KOMPAKT DİZ AYAK BİLEĞİ YARDIMCI ALET TASARIMI

Mehmet Furkan Baltacıoğlu

İleri Malzemeler ve Nanoteknoloji Programında Tezli Yüksek Lisans

Tez Danışmanı: Dr. Öğr. Üyesi Ramazan Ünal

Aralık 2018

Bu çalışmada yürüme, oturup kalkma ve merdiven çıkma için konsept yarı-aktif transfemoral protez tasarımı sunulmuştur. Bu çalışmada literatürde bulunan insan dataları analiz edilmiştir ve bu datalar doğrultusunda ilk olarak konsept dizayn sunulmuştur. Bu konsept dizayn 3 boyutlu yazıcı yardımıyla üretilmiştir. Bundan sonra, yapılmış olan model doğrultusunda çalışma modifiye edilmiştir. Ayrıca, protezdeki yaylar teorik olarak hesaplanmıştır. Yapısal parametreler doğrultusunda sonlu elemanlar metodu kullanılarak protez analiz edilmiştir. Ve protezdeki parçalar topoloji optimizasyon metodu kullanılarak yapısal olarak optimize edilmiştir.

Anahtar Kelimeler: Yardımcı Cihaz, Tasarım, Diz-Ayak Bileği, Yürüme

Acknowledgements

I want to thank Assistant Prof. Ramazan ÜNAL for his support. In my M. Sc. period he always motivated me. I really enjoyed by studying with him.

I want to thank Dr. Robert Riener for sharing the data of stair climbing.

Last but not least, I want to thank my mother, father and sister for their endless love and support. In my whole life, they are always with me. Without their invaluable encouragement, I couldn't accomplish this thesis.

Table of Contents

List of Figures

List of Tables

Huzurum, yaşam sevincim; biricik annem, babam ve kardeşime…

Chapter 1

Introduction

Because of traumas, tumor, infections, nervous and vascular system problems and some other reasons amputations of lower limb occurs [1]. On the other hand, an average adult person walks more than 5000 steps each day, except sportive activities [2]. Hence, bringing these people into active life is highly necessary, for this purpose assistive devices are widely used [3].

Assistive devices are used for people who have disorder or disease that prevents people to make their daily activities by themselves [4]. And as a type of assistive device, transfemoral prostheses are designed to replace knee and ankle joints of individuals who has above-knee amputation [5]. With the use of transfemoral prostheses these people can do their activities of daily life, i.e., walking [6], sitting, standing up by themselves [7]. Also, providing amputees to do these activities by themselves, can do these people physically and psychologically better [8].

The number of people who experience one upper or lower limb amputation per year is more than 150.000 in USA [9] . Prosthetic and orthotic equipment demand in Africa, Asia and Latin America was estimated as 30 million until 2010 [10]. And nowadays, all around the world, there are more than 35 million people who need prosthetic or orthotic services and the number of need will be increased [11]. So, the importance of designing and making accessible assistive devices is increased correspondingly.

Restoring the kinematic functions of amputeed knee and ankle is the main goal of an above-knee prosthesis [12]. There are three types of lower limb prostheses according to their actuation principle. They are active, passive and semi-active prosthesis [6,13–16].

Passive prostheses use energy of human by exploiting human dynamics and they don't have extra energy source. Additionally, passive prostheses have constant mechanical characteristics like constant elastic element coefficients. So they can't mimic real kinematics of joints of healthy person [15]. About 60% extra metabolic energy is consumed by a transfemoral amputee using passive prosthesis compared to that of an able-bodied person during normal walking [17]. Additionally, his/her hip joint on the amputated side takes the triple power and torque [18]. And the need for extra energy sources causes amputee person who uses passive prosthesis to consume more human energy and to have walking defects [14].

Active prostheses are actuated and they use DC motors, pneumatic or hydraulic actuators to provide needed energy in a controllable way. Thus, active prostheses have potential to mimic motions of healthy person with its controllable actuator [6,19-25]. However, active devices have challenges like weight, cost and need of energy source, thus, active devices have some limitations as lightweight and high-efficiency components are needed [14,26].

Since active and passive prostheses have some handicaps semi active prostheses were produced. Semi-active prostheses combine the characteristics of active and passive prostheses [15]. For some activities like stair climbing, passive prostheses needs additional power [27]. Therefore, to compensate the needed power, semi-active prostheses are used. Semi-active prostheses can also mimic human walking kinematics like active prostheses with relatively low cost [16].

In [28], design, modeling and tests of a foot-ankle prosthesis were presented. The prosthesis is an active below knee prosthesis. Prosthesis also exploits the human energy to reduce the energy needed from the energy source and by reducing energy source need, they aimed to decrease the weight. Additionally, the study contains the optimization process of actuators and some other parts of prosthesis. At the end of their study, by

testing prosthesis on a subject at specified gait speeds, they underlined that the study opened a way of next generations of their prosthesis.

In [19], a transfemoral prosthesis which is pneumatically actuated was designed according to 75 kg human data. For this design as minimum range of motion, they determined 110 ° for knee and 65° for ankle. For the ankle and knee joints, they used slider-crank mechanism. As design parameter knee joint had 86 Nm and ankle joint had 130 Nm maximum torque. They optimized the design by considering design parameters and after optimization; knee actuator had 125° range of motion and ankle actuator had 87° range of motion. They tested the prototype with the help of able-bodied test adaptor. The study was validated with the help of this test. They underlined that prosthesis could produce needed torque and the prosthesis was able to produce needed power with the help of designed system, moreover, the human gait pattern could be mimicked by the prosthesis closely.

In [12], a semi-active above-knee prosthesis which contains two hydraulic actuators. They claimed that, at walking and stair ascending cases the design was successful because knee and ankle designs of prosthesis produced correct positive energy. Also, ankle and knee joints didn't generate much power at the same time at stair ascending task. Also, ankle dorsiflexion could be provided by the prosthesis in swing phase.

In [29], design for energy regenerative prosthesis was presented. By using hydraulic components, they aimed to solve problems about producing positive work. In the study they modeled the design computationally to have optimum hydraulic control pattern for practical activities and simulated for practical activities to evaluate the performance of their study. Practical activities were chosen as walking, running and sit-stance-sit. As mentioned in the study, results demonstrated that, kinematics of the knee could be reflected by prosthesis when optimization of system was totally made. Also, they mentioned that one damper is not enough for all functional activities so, by using energy-storage elements and controlling them, results became better.

In [30], design of a transfemoral electromechanical prosthesis which contains electrical actuator, springs, power converters was presented. As underlined in the study, the system involved energy regeneration parts. In the study, ten subjects' walking data at

different speeds were used for optimization and they increased the performance of prosthesis with the help of this optimization. They claimed that the prosthesis could work without external energy cost for walking in theory.

In [31], the design of an electromechanical transfemoral prosthesis was described. The prosthesis was able to store and regenerate the energy thanks to DC motor, generator and supercapacitor. They proposed different configurations for the design. And they optimized the study by using Simulink models and the optimization was based on biogeography. As mentioned in the study, their optimization model was able to provide tracking errors in the desired region.

In [32], H. A. Bayram, studied on novel progresses in lower-limb prostheses and also drew attention on the usage of springs in prosthetics design. It was emphasized that there was no commercialized prosthesis that can replicate able body kinematics which require more positive energy. Moreover, it was underlined that, novel studies focused on spring-based mechanisms to make energy stream efficient and controllable.

R. D. Belmann et.al designed a 2.1kg transtibial ankle prosthesis which is active and the design had two degree-of-freedom. 2 Dof was composed of inversion-eversion and plantarflexion-dorsiflexion. The design had the ability of running and jumping also. For these activities they used DC motors, springs, roller screws also [33].

Furthermore as underlined in [12], there are commercially available prostheses like Safety Knee [34], 3R80 Knee Prosthetic [35], C-Leg [36], Rheo Knee [37], Ossur Power Knee [38].

R. Unal et. al. designed a passive prosthesis which was capable of walking without needing external energy input and the prosthesis was capable of delivering needed energy for push-off at the ankle joint [39–42]. Moreover this prosthesis was modified later, and the new prosthesis could be used for different walk paces by changing the energy storage ability [43]. On the other hand, as the study of R. Unal et al. supports the reality that ideally walking does not require external power source [44, 45]. However stair ascending task requires external power source [46,47].

Under the light of literature, the aim of this study is designing a conceptual semi-active prosthesis which is capable of walking with weight acceptance, sit-to-stand and stair climbing. This new conceptual design will be called as WalkMECH V2, WalkMECH [48] was capable of walking and it was a fully-passive transfemoral prosthesis. Main objective of this study is designing the prosthesis as possible as passive and when the external power is needed, adding active parts which will make the design semi-active. As underlined in the literature, this will make the prosthesis light and combine the best properties of passive and active prosthesis.

Chapter 2

Data Analysis

To be able to make a prosthesis that is used for walking, sit to stand and stair climbing, human data need to be analyzed. In this chapter, data analysis that contains walking, sit to stand and stair climbing is presented by using healthy human data. The main purpose of this study is designing and developing a prosthesis that can mimic healthy people activities by means of elastic elements, locking mechanisms, engage-disengage mechanisms.

2.1 Human Gait, Sit to Stand and Stair Climbing

2.1.1 Human Gait

As a methodology, one human gait cycle starts with the touch of a foot to the floor. Then one human gait cycle is considered to be 100 percent. One human gait cycle is composed of two main phases. First of them is stance phase which refers to foot contacts to the floor and the second one is swing phase which means foot does not contact with the floor anymore and foot will contact with floor after this phase [49]. Swing phase and stance phase of walking are shown as grey on subject foot which is depicted above, in Figure 2.1.1.1.

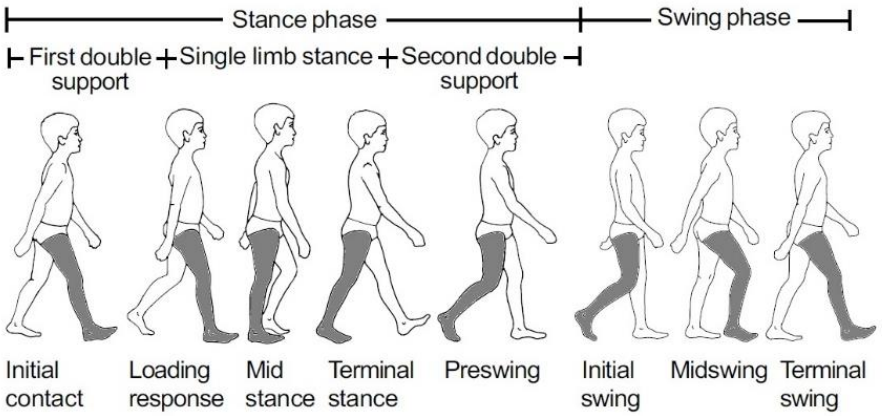

Figure 2.1.1.1 Phases and events of walking on an image. Adapted from [49] with permission.

Stance phase include five events, they are initial contact, loading response, mid stance, terminal stance and preswing. Initial contact starts the human gait cycle and, in this phase, heel strikes to the ground. During loading response, the foot becomes parallel to the floor. After that, as the stance foot becomes at the behind of swinging foot, midstance occurs. While terminal stance takes places, heel of the foot starts to separate from floor and human starts to push off his/her foot from the floor. In preswing foot looses its contact to the floor (toe-off) and ends the stance phase and totally, stance phase takes place between 0% and 60% of the gait cycle [50].

Swing phase contains three events as initial swing, mid swing, terminal swing. Initial swing starts after the toe-off phase. And person move leg forward after this event. Midswing occurs as the swinging foot passes the opposite foot. Before the next gait cycle, in terminal swing subject slowdowns his/her leg for the first floor contact. Totally, swing phase takes place between 60% and 100% of the gait cycle [50].

To summarize phases and 100% of human gait, Figure 2.1.1.2 and Table 2.1.1.1 can be are presented. Figure 2.1.1.2 represents the human gait by using rotating wheel. Table 1, contains angle values of the gait cycle, i.e., hip, knee and ankle joint angles for human gait.

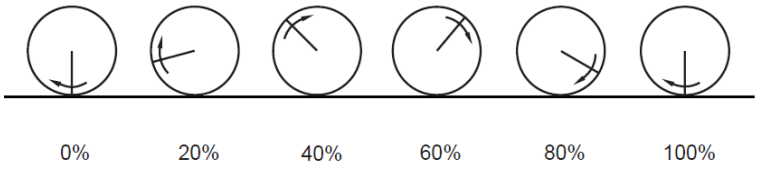

Figure 2.1.1.2. Rotating wheel, represents the human gait cycle. Reprinted from [49] with permission.

	Stance Phase					Swinging Phase		
Gait Phases	Initial Contact	Loading Response	Mid Stance	Terminal Stance	Pre Swing	Initial Swing	Mid Swing	Terminal Swing
Gait Cycle	0 %	0 – 12 %	12 – 31 %	31 – 50 %	50 – 62 %	62 – 75 %	75 – 87 %	87 – 100 %
Hip	20° flexion	20° flexion	0° flexion	-20° hyper extension	-10° hyper extension	15° flexion	25° flexion	20° flexion
Knee	0° – 5° flexion	20° flexion	0° – 5° flexion	0° – 5° flexion	40° flexion	60° – 70° flexion	25° flexion	0° – 5° flexion
Ankle joint	0°	5° – 10° plantar flexion	5° dorsal flexion	10° dorsal flexion	15° plantar flexion	5° plantar flexion	0°	0°

Table 2.1.1.1. Hip, knee and ankle joint angles for human gait. Adapted from [51] with permission.

To explain the power, angle and moment change in the knee and ankle Figure 2.1.1.3 is presented. Figure 2.1.1.3 contains the angle, moment and power graphics of the ankle and knee joints.

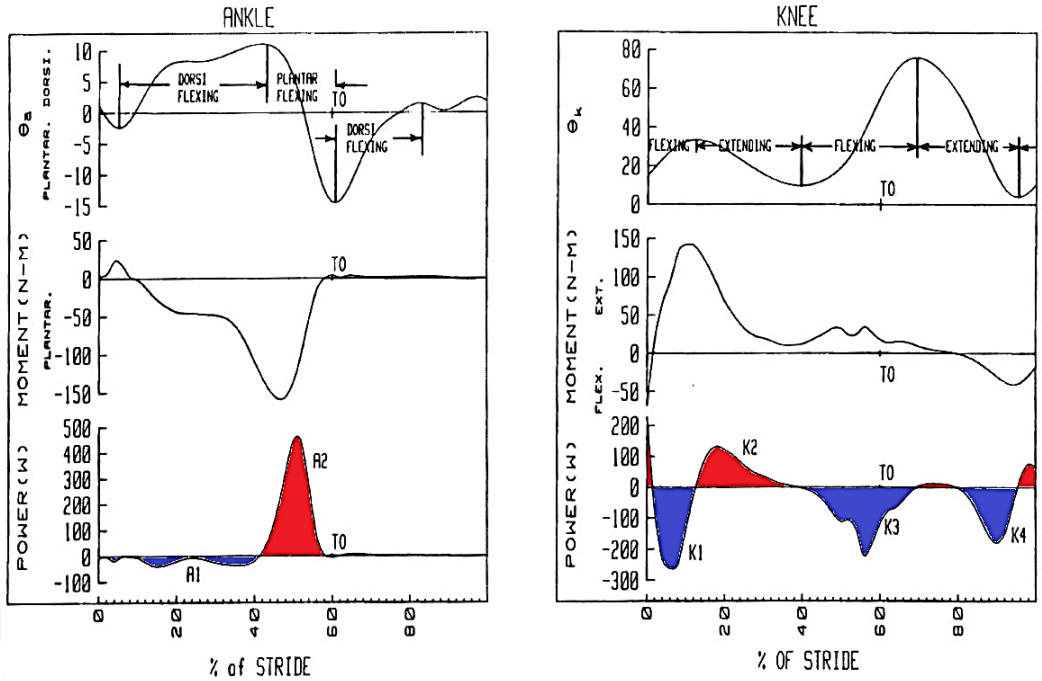

Figure 2.1.1.3 Power, moment, angle values of the ankle and knee vs walking strides. Adapted from [52].

By considering Figure 2.1.1.3 left side, while moment about ankle joint is positive, between 0%-5% of gait cycle, foot makes plantarflexion movement. At the end of this interval, result power is very limited. Between 5%-40% of gait cycle foot makes dorsiflexion movement and meantime moment about ankle joint is negative (plantar flexion moment). As a result, A1 power area which is shown as blue on graphic is formed. And this area is energy absorption area. Also, between 5%-40% of gait cycle, especially after 35% of gait cycle, moment is increasing in negative way for heel-off case. Between 40%-60% of stride A2 power area which is shown as red on graphic is formed. Toe off happens at 60% of gait cycle. After this point, the moment becomes nearly zero and ankle dorsiflexes [52].

By taking into account Figure 2.1.1.3 right side, between 0%-15% of gait cycle knee makes flexion movement and this part produces K1 energy area which is shown as blue. This energy is negative so, it is energy absorption area. After 15% of gait cycle, between 15%-40% of gait cycle, knee makes extension movement and red K2 energy area is arisen. This energy is positive so, this is energy generation area. And the amount of energy in this area, is about 10% of total generated energy while walking. Between 40%-70% of gait cycle, knee makes flexion movement and K3 energy area is formed. This area is showed as blue in graphic. And this area is negative energy area which means energy

absorption area. Toe-off takes place in this interval. After 70% of gait cycle, knee extends. Meanwhile, K4 energy area is formed. This area is shown as blue and this area is energy absorption area [52].

2.1.2 Sit to Stand

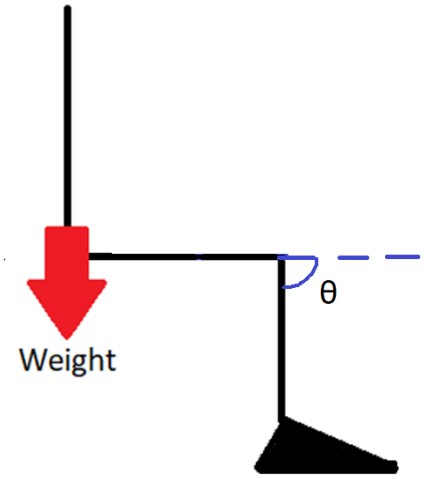

Figure 2.1.2.1 Changing angle while sit to stand process

Sit to stance can be described as a person's standing up event from sitting position. Meanwhile θ angle as shown in Figure 2.1.2.1, starts from 90° and decreased to 0°. In this process, big amount of torque is provided by knee joint. To calculate the torque about knee joint, eqn (2.1.2.1) was used.

$$M_{knee} = m * g * l * \sin(\theta) \qquad (2.1.2.1)$$

In this equation m represents the weight of the body concentrated at hip joint. The weight at this point was accepted as 25 kg for one leg. g represents the gravity constant as 9,81 m/s^2. l is the distance between the knee joint and hip joint, which is equal to 0,45m. After these recognitions, knee angle vs torque graphic as it is depicted in Figure 2.1.2.2.

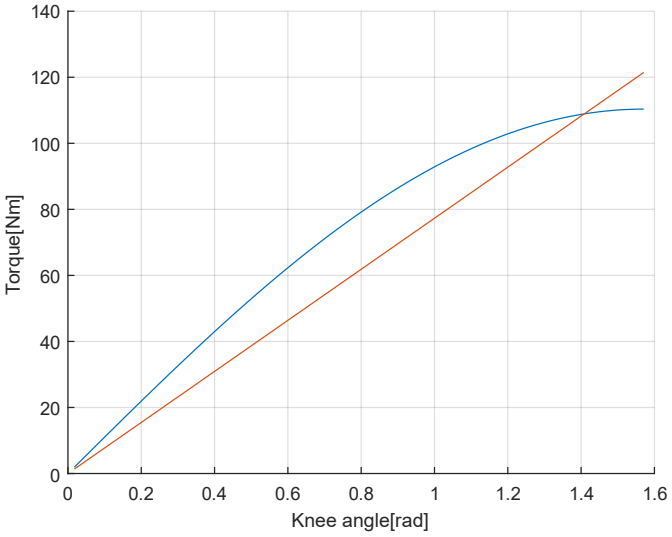

Figure 2.1.2.2 Torque vs angle graphic of knee while sit to stance

Torque about knee joint is not changing linearly for increasing angle as it is shown as continuous blue line on Figure 2.1.2.2. But assuming the behavior of this condition as linear helps us, in design for sit to stance. As a consequence, graphic of sit to stance transformed to linear as it is seen with continuous red line on Figure 2.1.2.2. In this plot, while subject starts to sit down, torque is minimum. And after that, with increasing angle, torque increases correspondingly.

2.1.3 Stair Ascending

The moment change about knee joint can be explained with the help of Figure 2.1.3.1 for stair ascending. In the figure, moment change in knee joint correspond to angle of knee is shown. 0% corresponds to the first contact of foot to the floor. After this point, because of weight of human, moment increases greatly about knee joint as it is shown in the figure. Thereafter, moment takes the highest value of all process about 18% of stride. Then, after this peak point, moment starts to decrease. In figure, about 60% of stride, toe off takes place. After toe off, leg swings. While swinging, moment stays low and fluctuates. Just like behavior of moment, in the starting phases of stair climbing, huge amount of power is produced which is about 2,5W/kg by knee because body raises. After that, especially after toe off, power fluctuates and then becomes nearly zero [53].

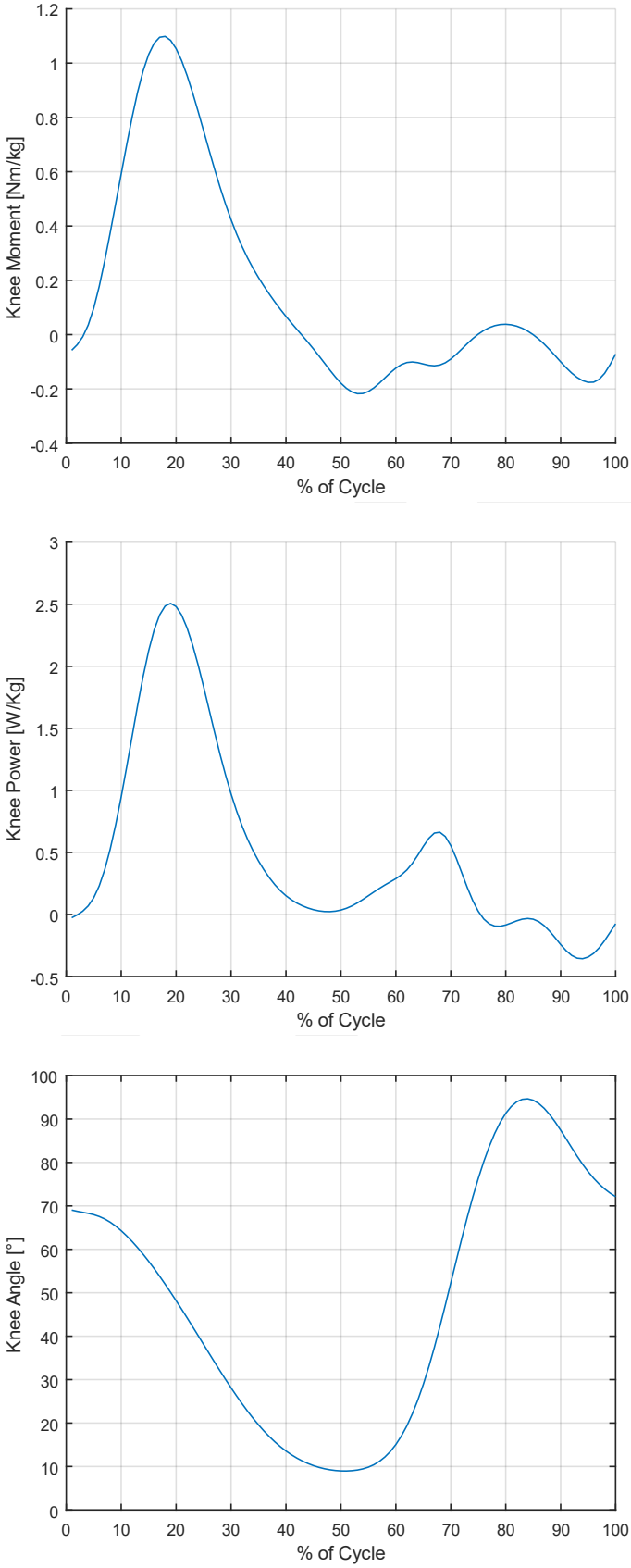

Figure 2.1.3.1 Moment, power and angle vs stride of stair ascending for the knee joint [53].

Chapter 3

Conceptual Design and Structural Analyses of an Energy-Recycling Transfemoral Prosthesis for Activities of Daily Life

** This chapter has been partially published in Proceedings of 18th International Conference on Machine Design and Production, UMTIK 2018.*

In this chapter, conceptual design of a semi-active prosthesis that can provide walking, stair climbing and sit to stand activities was described. The conceptual design is the second phase of WalkMECH [48] which was able to provide needed push-off power at ankle joint during walking and it was a fully-passive transfemoral prosthesis. This prosthesis is a semi-active prosthesis utilizing elastic elements to regenerate the energy when it is needed. In this chapter, the design was improved to make prosthesis being able to do weight acceptance with a knee flexion, sit to stand and stair climbing activities. The design was made according to human data which are depicted in Chapter 2. Firstly, CAD model of conceptual design is presented and then, structural analyses were made for the knee and ankle compartments.

3.1 Design

3.1.1 Design Specifications

Conceptual design of prosthesis which was designed under the light of literature and data analysis, and also its working principle are described in this chapter with the help of Figure 3.1.1.1.

Requirements of design was configured according to 1.80m height and 80kg weight person. According to these design specifications, CAD design of conceptual design was made. As it was depicted in the introduction chapter, a fully passive prothesis for walking can be made [44,45]. Studies in the literature support this reality like Unal Et al [39–42]. Still other than walking like stair climbing activity requires external power source [46,47]. Additionally, by taking into account biomechanical data, in this design range of motion of the knee joint is 0°-100° and range of motion of ankle joint is 20° dorsiflexion and 40° plantar flexion.

Figure 3.1.1.1 CAD Model of Conceptual Design

3.1.2 Working Principle of Weight Acceptance

With the help of the first elastic element as shown as ’1’ in Figure 3.1.2.1, the knee and ankle joint are connected energetically. In this study this spring will be called as coupling spring. The second elastic element as shown as ‘2’ in Figure 3.1.2.1, is used for weight acceptance purpose. This elastic element does weight acceptance in stance phase. The third elastic element as shown as ‘3’ in Figure 3.1.2.1, is used for energy storage in the ankle in stance phase. The fourth elastic element as shown as ‘4’ in Figure 3.1.2.1, is the part of catapult mechanism and it is used to assist for effective and sufficient push-off.

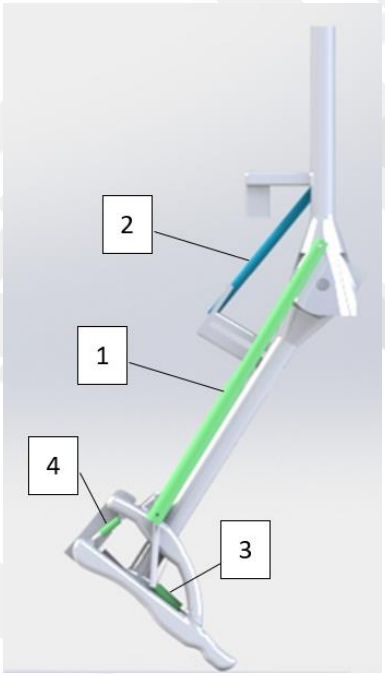

Figure 3.1.2.1 Elastic Elements of Conceptual Design

All these elastic elements and their working principles are shown in Figure 3.1.2.2. In this figure, while elastic elements store the energy they are shown as red, and while they release their stored energy they are shown as green. Moreover, when they are unloaded, they are shown as blue in Figure 3.1.2.2.

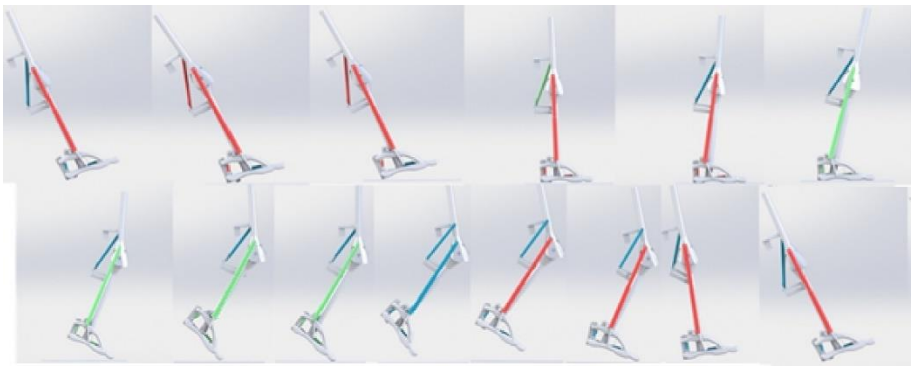

Figure 3.1.2.2. The working principles of the elastic elements during walking - the upper part shows the stance phase and the lower part shows the swing phase.

In Figure 3.1.2.3, the elastic element which is used for weight acceptance is seen as '2'. It is also shown as the second elastic element in Figure 3.1.2.1. This elastic element allows knee flexion during stance phase also at the same time, the moment caused by weight acceptance is mimicked by this element. The weight acceptance elastic element is active only during weight acceptance. And it is disabled with the mechanism as shown in Figure 3.1.2.3. As the mechanism, shown in Figure 3.1.2.3, touches the ground, weight acceptance is started as shown in Figure 3.1.2.3 center and when heel looses its contact with floor, the mechanism disengages the spring.

Figure 3.1.2.3 Weight acceptance mechanism and elastic element

3.1.3 Working Principle of Sit to Stand

For sit to stand function, the same principle of weight acceptance was used. Thus, it was aimed to provide sit to stand function with the help of one elastic element. For this function an elastic element which is parallel to weight acceptance elastic element was used. This elastic element stores the energy until 100° flexion of the knee and after 20°

flexion, engages the second elastic element. The elastic element is locked during sit phase as shown in Figure 3.1.3.1(center) to ensure the safety.

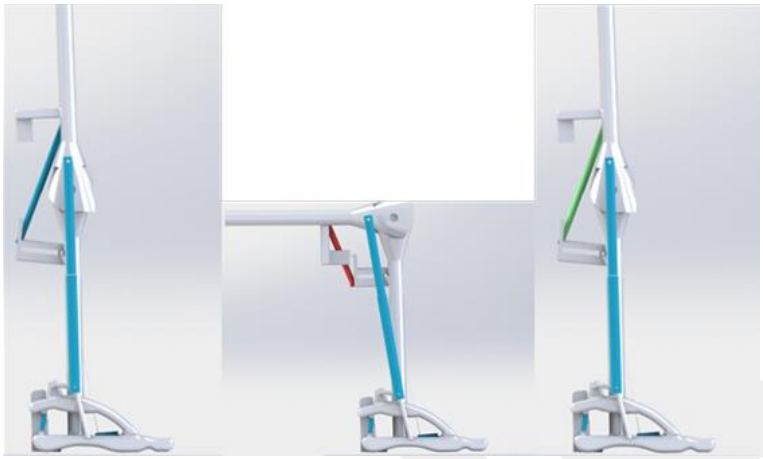

Figure 3.1.3.1 Working Principle of Sit to Stance Elastic Element (blue-unloaded, red-stored energy, green-releasing the stored energy)

3.1.4 Working Principle of Stair Climbing

As emphasized in the previous chapter, external energy needs to be applied to knee for stair climbing function [46,47]. For this purpose, as it is seen in Figure 3.1.4.1., the elastic element is compressed with the help of motor with ball screw mechanism.

Figure 3.1.4.1 Ball-screw mechanism, motor and elastic element for stair-climbing function

Because stair climbing activity takes more time compared to other activities especially walking, low-power motor can be used to compress the spring that is used for

stair climbing and by means of this mechanism extra energy can be stored on stair climbing elastic element. And this low-power motor would be useful for different speeds and inclination adaptation. This system is shown in Figure 3.1.4.2 and also working principle is shown in Figure 3.1.4.2 during stair climbing.

Figure 3.1.4.2 Stair climbing function of conceptual design

3.1.5 Working Principle of Catapult Like Mechanism

Main purpose of the catapult mechanism is assisting the effective and sufficient push-off. For this purpose, the catapult like mechanism was designed as shown in Figure 3.1.2.3. As the weight of human is applied on mechanism the springs between upper side and lower side of foot are compressed and meanwhile at stand phase of walking, the mechanism is locked with the help of locking mechanism as shown in Figure 3.1.5.1. After that, at push-off phase, it releases the stored energy.

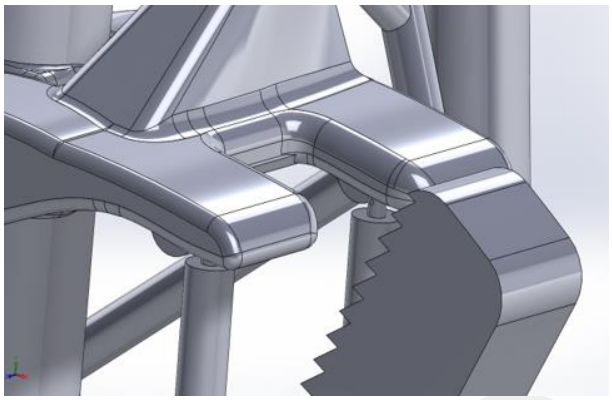

Figure 3.1.5.1 Locking mechanism of catapult like foot compartment

3.1.6 Working Principle of Coupling Spring

Working principle of the coupling spring was shown in Figure 3.1.2.2. The coupling spring stores the energy and at push-off phase it starts to release the stored energy. And also, this spring is used for knee flexion movement to prevent the prosthesis touch to the floor in swing phase.

The knee joint was designed as shown in Figure 3.1.6.1 to prevent the knee from hyper-extension. Moreover, the joint was designed within the dimensions of biological knee as shown in Figure 3.1.6.1.

Figure 3.1.6.1 CAD design of knee

Catapult-like ankle-foot compartment of the prosthesis was designed according to the natural foot of human by using Solidworks as shown in Figure 3.1.6.2.

Figure 3.1.6.2 CAD design of catapult like ankle-foot compartment of prosthesis

3.2 Structural Analysis

In this section structural analyses of the knee and ankle parts of the prosthesis are presented. The analysis was made in ANSYS environment. Since AL 7075-T6 is accessible and free machining material and also has low-weight, high strength [54] , AL 7075-T6 is used for assistive devices [55]. Therefore, in this study for structural analysis AL 7075-T6 material was used as a candidate material.

3.2.1 Catapult Like Ankle-Foot Compartment

The ankle-foot compartment design is composed of frame, springs, locking mechanism, energy transfer mechanisms to regenerate energy and catapult mechanism. The foot-ankle compartment is composed of two main frame parts for catapult mechanism. One of them is upper side of the foot and the other one is lower part of the foot. The sole part of the foot is presented in Figure 3.2.1.1.

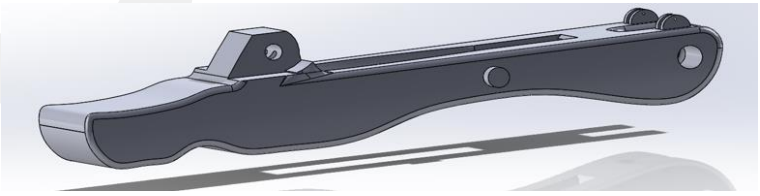

Figure 3.2.1.1 Sole Part of foot-ankle compartment

The lowerpart (sole of foot) was modeled by using Solidworks according to the natural human foot size which was accepted as 30*10 cm. The length of the foot is 30cm and the width of it is 10cm as shown in Figure 3.2.1.2.

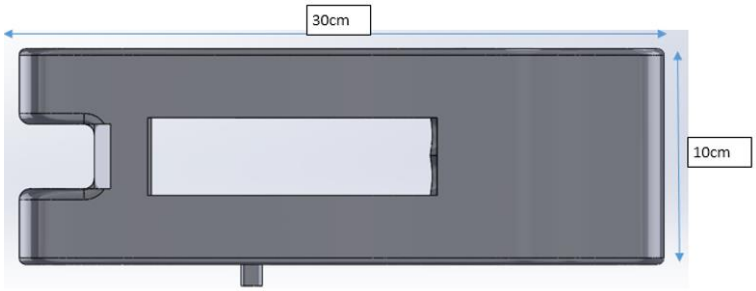

Figure 3.2.1.2 Size of sole part of foot-ankle compartment

As shown in Figure 3.2.1.3 finger part of foot is placed after catapult mechanism, so they do not interfere with each other. The design of catapult like ankle-foot compartment is shown in Figure 3.2.1.3 and Figure 3.2.1.4.

Figure 3.2.1.3 CAD design of foot-ankle compartment

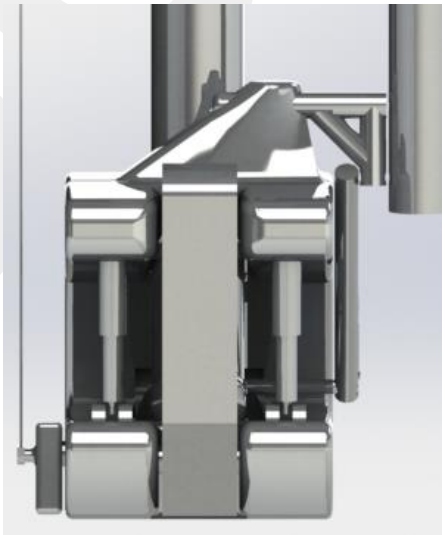

Figure 3.2.1.4 CAD design of foot-ankle compartment from behind

To decide the shape of upper side of foot, two different feet model were designed. These feet have similar dimensions and have same materials. Lower parts of the foot are same but the trajectories of upper side of feet are different as shown in Figure 3.2.1.5. Feet were designed in Solidworks. Their models were analyzed by using Ansys Static Structural tool. In FEM analysis, applied force on parts was 784,8N (80kg*9,81m/s^2) which is the weight of human body.

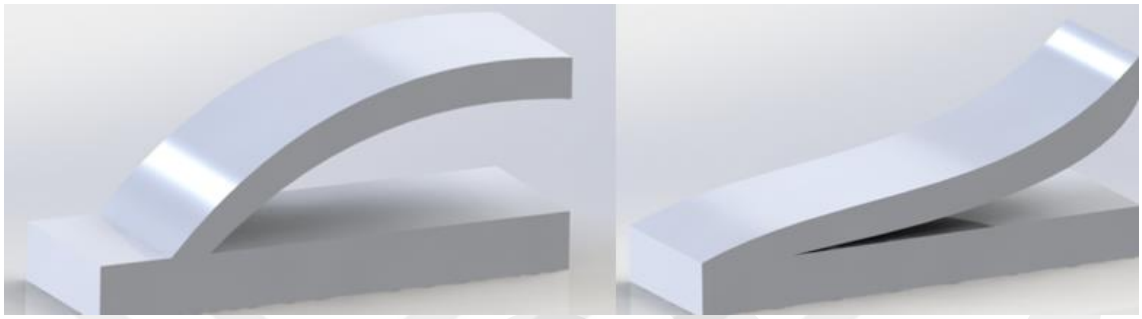

Figure 3.2.1.5 Foot candidates of design

After applying forces as shown in Figure 3.2.1.6, stress and deformation analyses of parts were resulted as shown in Figure 3.2.1.7.

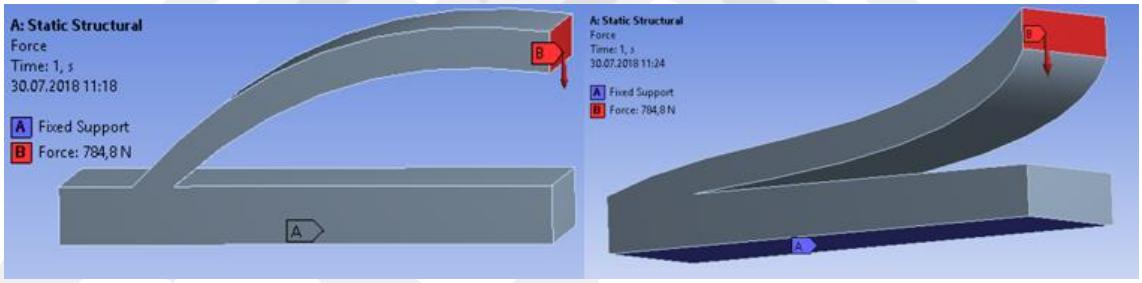

Figure 3.2.1.6 Applied Forces of Form 1 and Form2

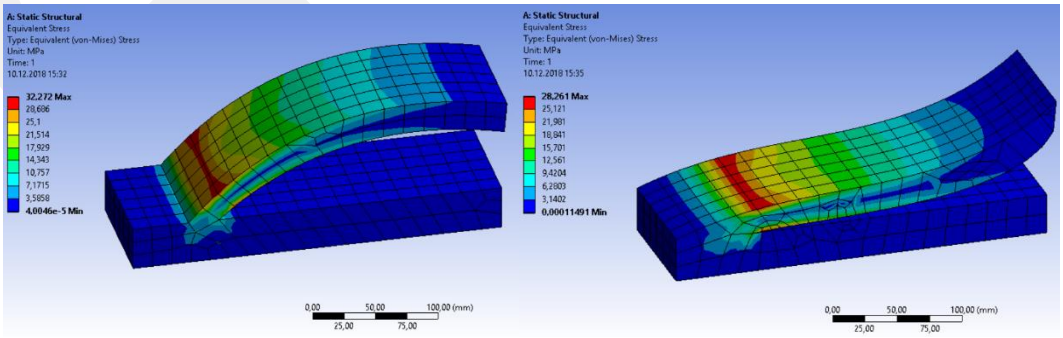

Figure 3.2.1.7 Stress results of form1 and form2

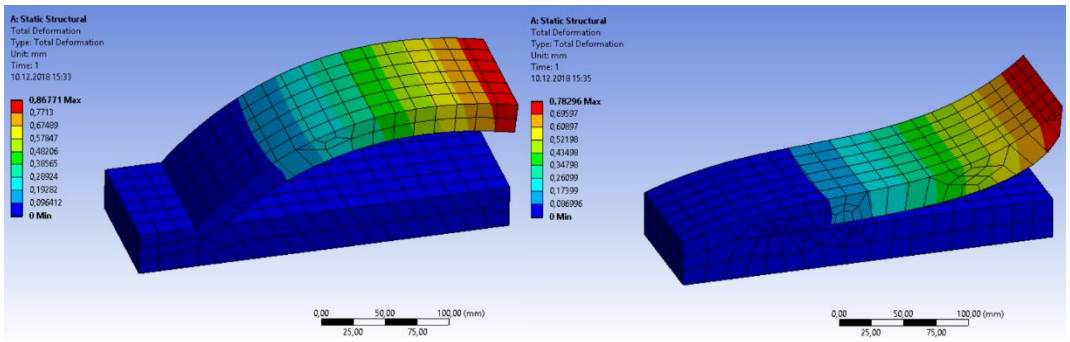

Figure 3.2.1.8 Deformation results of form 1 and form 2

According to results as shown in Figure 3.2.1.7 and Figure 3.2.1.8, deformation analyses are close each other. Additionally, stress values of the forms are close each other but critical areas which are seen as red color in Figure 3.2.1.7 are more on the right candidate especially at the connection of upper side and sole of the foot. Moreover, for springs and other parts of prosthesis the area in foot is more convenient on the left candidate. By considering the results, the left candidate was chosen for design.

By considering critical regions on foot in Figure 3.2.1.7, the design was modified as shown in Figure 3.2.1.9. In this process, radius was set to intersection of upper part and lower part of foot. Locking mechanism's place was modified. Also, foot was modified according to natural human foot. In Figure 3.2.1.9, deformation and stress results of the modified foot are depicted. These analyses represent the push-off phase that has the maximum stress for the finger part of foot. These results are acceptable.

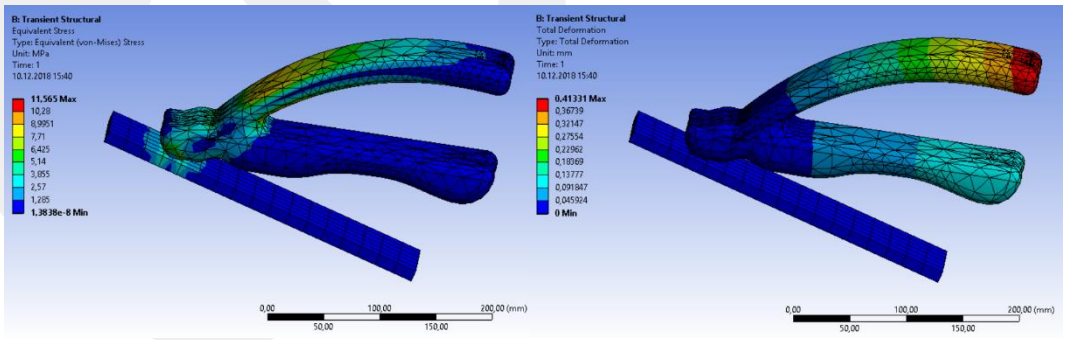

Figure 3.2.1.9 Stress and deformation results of modified foot-ankle compartment

After the modification of foot as shown in Figure 3.2.1.9, the place of rollers were added on design and for rollers, the thickness of parts was increased and upper side of foot was analyzed separately. The applied force on the part is same with previous analyses as shown in Figure 3.2.1.6, Figure 3.2.1.7 and Figure 3.2.1.8. At this point, because the

weight of leg taken into account, safety factor was increased. Stress and deformation analyses results are shown in Figure 3.2.1.10. The stress distribution is more or less symmetrical and acceptable.

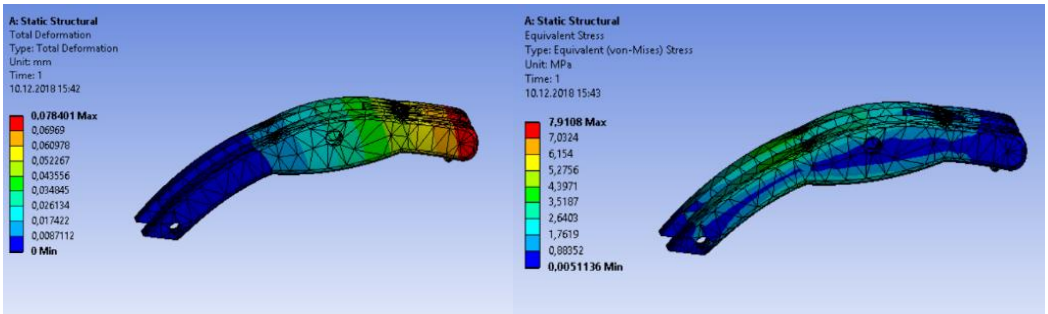

Figure 3.2.1.10 Stress and deformation results of upper side of foot-ankle compartment

3.2.2 Knee Design

In the process of the knee joint analysis, knee was analyzed as two parts that are lower and upper parts of the knee. Firstly, upper side of the knee was analyzed. Following that, the part was modified by using analysis results. In Figure 3.2.2.1 left side, the initial model of the knee is depicted. In the analysis, the applied force is the force that is generated by the weight of human and stair climbing activity because it has the highest torque in motions as shown in chapter 2. According to analysis results, the connection areas of the upper link and the knee is given as red and these red areas are local critical areas. So, according to results, the knee was modified and shown in at the right side of Figure 3.2.2.1. Radius was set to connection areas of the upper link and knee because it has critical regions. Also, side parts of the knee were thickened while modifying. Ansys analysis was repeated for modified part as it is shown in Figure 3.2.2.1 right side, the maximum stress was decreased and stress is acceptable.

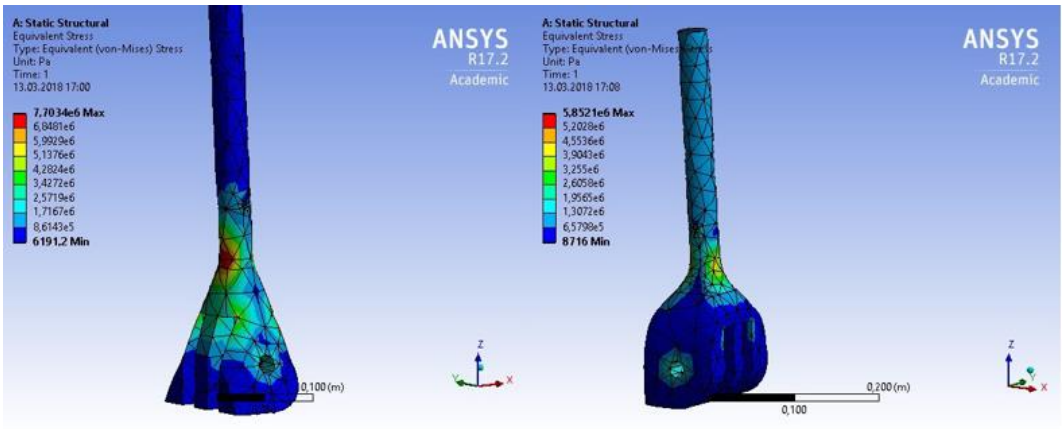

Figure 3.2.2.1 Structural analysis of upper part of knee

Similarly, the bottom part of knee was analyzed in Ansys environment. As shown in Figure 3.2.2.2, distribution is smooth and safe. Although this part is seen as over safe, since this part works with upper part of knee and to prevent hyper-extension of the knee this part was not modified.

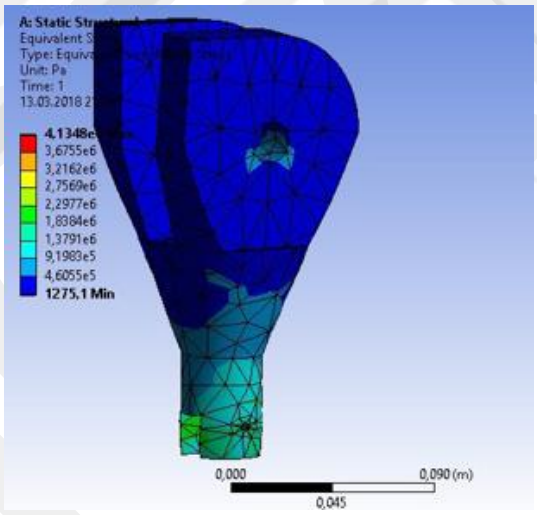

Figure 3.2.2.2 Structural analysis for lower part of knee

Moreover, in this study, initial prototype of the conceptual design was built by using 3D printer. This prototype is helpful for visualizing the mechanisms and developing the next generation of prototype, especially in the point of manufacturing. Also, the prototype would be useful to open new perspectives on design. 3D printed initial conceptual design is shown in Figure 3.2.2.3 and it is half-scale prototype made with PLA material.

Figure 3.2.2.3 3D printed prototype of conceptual design in half-scale

3.3 Results

In this chapter, new conceptual design of WalkMECH [48] is presented. And this conceptual version of WalkMECH is capable of weight acceptance, sit-to-stand, stair climbing. Firstly, human biomechanical data were analyzed and according to data, working principles of elastic elements on prosthesis were designed and presented. Then structural analyses of the knee and ankle compartments were implemented. For structural analyses, it was aimed to observe the optimum trajectories. So, according to the structural analyses, it is clear that, the design is not optimum in terms of structural and mechanisms yet, so for this purpose in next chapters, optimizations of structural parts and mechanism will be described.

Chapter 4

WalkMECH 2.1: Design of an Energy-Recycling Transfemoral Prosthesis for Activities of Daily Life

* *This chapter has been partially presented in International Biomechanics Congress, BIOMECCON 2018.*

In this section, new conceptual design of WalkMECH 2.0 is presented. This conceptual design is the next generation of Walkmech 2.0 which is explained in chapter 3. And the new conceptual design is called as WalkMECH2.1. In this version, design was partially changed to make the prosthesis more compact and also with the help of 3D printed conceptual design WalkMECH 2.0, mechanisms were optimized to let them work smoother and safer. The design has the ability of weight acceptance during walking, sit to stance and stair climbing. For these abilities firstly, biomechanical data were taken into account and then the WalkMECH 2.0 was modified to 2.1 version. In this chapter, changed mechanisms and designs are described and also coefficients of elastic elements and motors are presented. Furthermore, the changed CAD design of the prosthesis is presented.

4.1 Design

4.1.1 Weight Acceptance Spring

To apply weight acceptance mechanism to the design it should be underlined that the highest torque about the knee while walking is occurred in weight acceptance [52]. As it is seen from Figure 2.1.1.3, the increase and decrease manner of torque during weight acceptance is nearly linear [52]. So, with the help of an elastic element, this behavior can be mimicked. The task of this elastic element during walking is shown in Figure 3.1.2.2 and Figure 3.1.2.3. It was seen with the help of 3D printed model of WalKMECH2.0 that, place of weight acceptance elastic element could be problematic because it was placed behind the prosthesis and it could fail during activities and also it was not seem to be compact which is one of the main motivation points of this study. So, the place of weight acceptance elastic element changed and shown in Figure 4.1.1.1.

Figure 4.1.1.1 Weight acceptance elastic element

According to the place of spring, weight acceptance spring coefficient was determined. To do that, firstly elongation versus spring force graph was gathered by using the needed knee torque. The graph is shown in Figure 4.1.1.2. As it is shown in Figure

4.1.1.2, there are two different elastic element characteristics during gait. The first one which has high slope, shows the knee behavior during weight acceptance elastic element and the second one which has low slope, shows the knee behavior of push-off and swing phase of gait. To find the coefficient of weight acceptance elastic element, high slope part was taken into account and with the help of the line, as shown as red on Figure 4.1.1.2, coefficient of the elastic element was found.

$$k_{WA} = \frac{1038 - (-137{,}5)}{15{,}82 - 6{,}691} = 128.77\ [N/mm] \qquad (4.1.1.1)$$

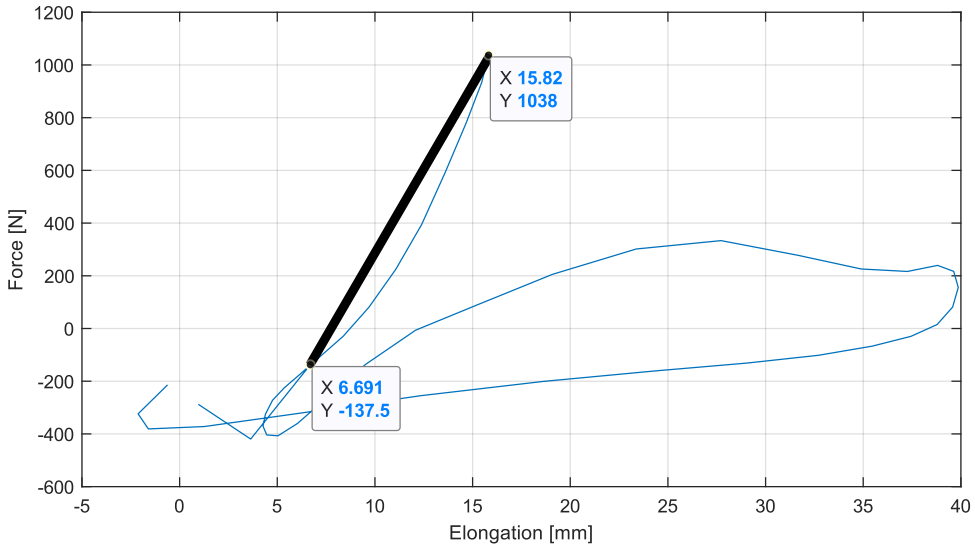

Figure 4.1.1.2 Force vs elongation graph of weight acceptance elastic element

4.1.2 Sit to Stand Spring

For sit to stand activity, the elastic element was modified from Figure 3.1.3.1 to Figure 4.1.2.1. The mechanism is started manually by the user and the spring coefficient is constant. The used elastic element is torsional spring and energy transfer mechanism is connected to the knee joint. Here the locking mechanism which ensures that the mechanism is locked at sitting case, was changed also. In Figure 4.1.2.1 the locking mechanism is shown as red. User locks the rotation of the knee by using this shaft manually and when the user starts to standing up, user releases the knee by pulling this shaft.

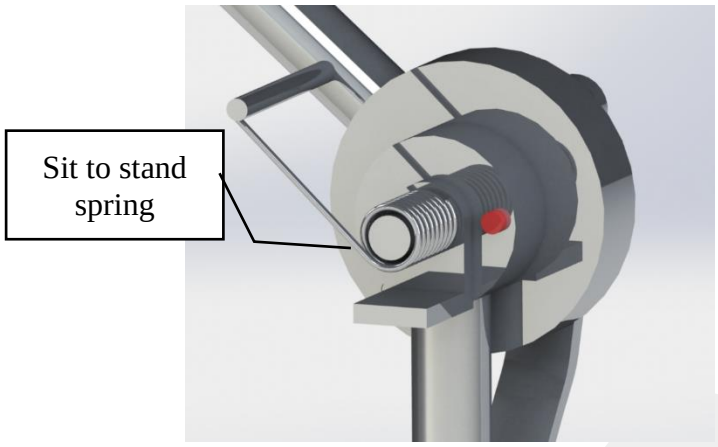

Figure 4.1.2.1 Sit to stand spring

By using Figure 4.1.2.2 sit to stand spring coefficient was found. To find the coefficient, the slope between two points, shown in Figure 4.1.2.2, was calculated as (4.1.2.1).

$$k_{Sit\ to\ Stance} = \frac{105 - 26.7}{1.257 - 0.2443} = 77.32\ [Nm/rad] \quad (4.1.2.1)$$

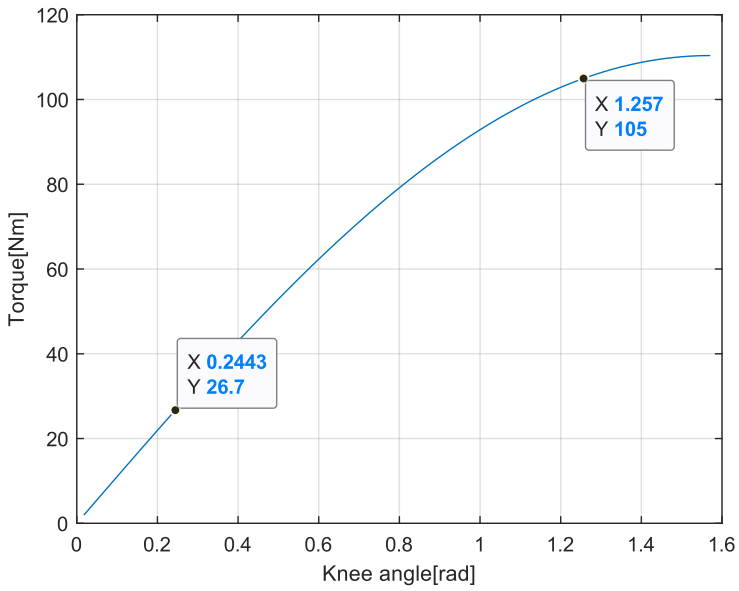

Figure 4.1.2.2 Torque vs angle difference graph of sit to stand spring

4.1.3 Stair Climbing Spring

For stair ascending activity, an actuator was implemented and the design modified from Figure 3.1.4.2 to Figure 4.1.3.1. The actuator system contains spring and a dc motor. In this point, minimizing the dc motor is the main focus. So, ascent data was analyzed and spring was determined.

Figure 4.1.3.1 Stair ascending actuator and elastic element

To decide the stair ascending spring, force vs elongation of elastic element was generated. The Figure 4.1.3.2 shows the force vs elongation behavior of spring.

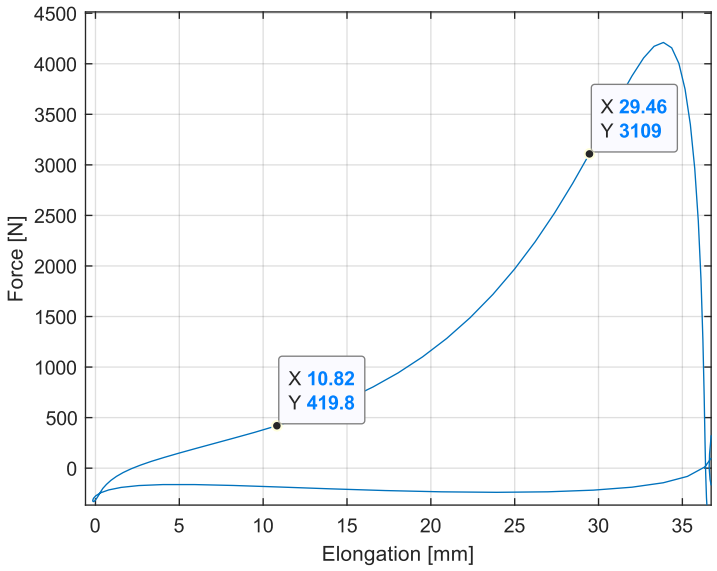

Figure 4.1.3.2 Force vs elongation graph of stair ascending elastic element

As it seen from Figure 4.1.3.2, there are two different phases on graph. The first one, with higher slope, gives the data about knee during stair ascending. And the second one, with lower slope, gives the data of swing motion of leg. In this figure, line between the points, marked as square, gives the coefficients of stair climbing spring. The slope of the line can be found with the help of eqn (4.1.3.1).

$$k_{Ascent} = \frac{3109 - (419.8)}{(29.46 - 10.82)} = 144.27\ [N/mm] \qquad (4.1.3.1)$$

4.1.4 Weight Acceptance Spring in Foot Compartment

The working principle of catapult mechanism was depicted in title 3.1.5. Here, springs of the weight acceptance spring in foot compartment will be described. Positions of the springs are shown in Figure 4.1.4.1.

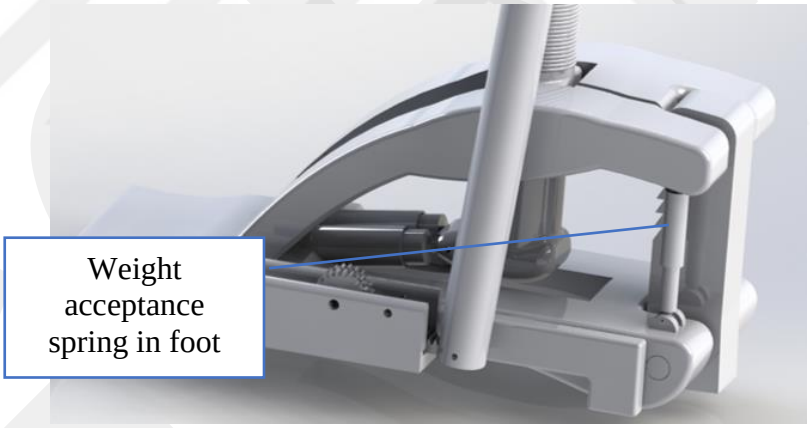

Figure 4.1.4.1 Weight acceptance spring in catapult mechanism

To decide the spring compression value, the system was analyzed in CAD program. Here, configuring the distance between floor and ankle joint equal to that of healthy ankle is the main decision criteria. Thus, the spring compression value is calculated as 4 mm. The forces on the foot compartment was calculated as shown in Figure 4.2.1.2 and eqn. (4.1.4.1), (4.1.4.2) , (4.1.4.3).

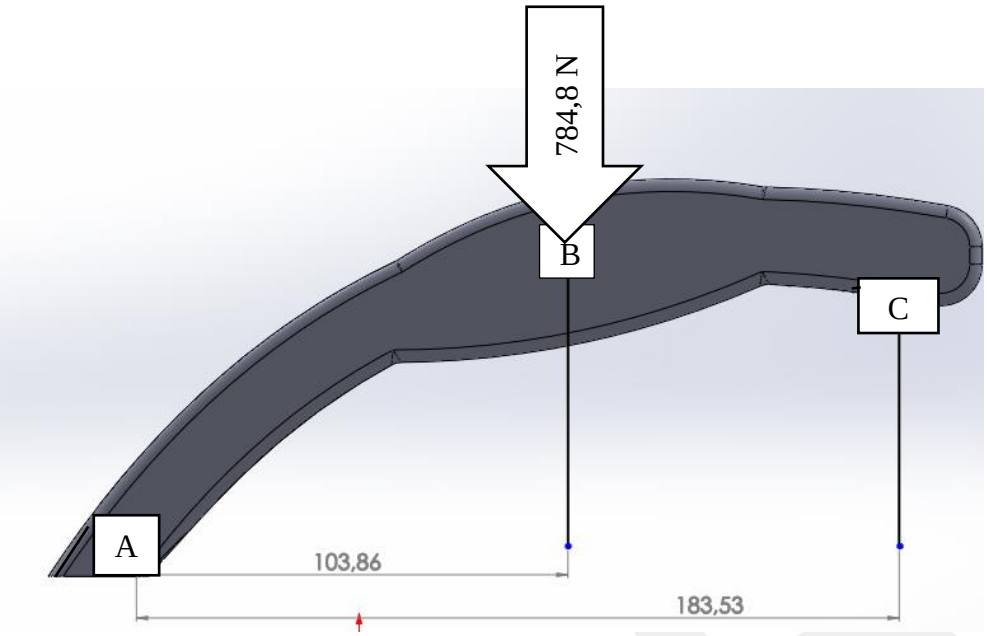

Figure 4.1.4.2 Force and place of joints for spring on upper side of foot.

Maximum total vertical force on the floor contacted foot can be calculated as;

$$F_B = 80kg * 9.81m/s^2 = 784{,}8\ N \tag{4.1.4.1}$$

With the help of moment about point A, maximum F_C was calculated;

$$\sum M_A = -784{,}8N * 103{,}86mm + F_C * 183{,}53mm = 0 \tag{4.1.4.2}$$

$$F_C = 444{,}12\ N \tag{4.1.4.3}$$

Force on springs is 444,12 N. For each springs the force is 222,06N. Therefore, the spring coefficient was calculated as shown in eqn (4.1.4.4).

$$k_{spring} = \frac{222{,}06}{4} = 55{,}51\ N/mm \tag{4.1.4.4}$$

4.1.5 Ankle Spring

The task of this elastic element is supplying the needed energy for push-off phase. For this purpose, the ankle spring stores the energy in dorsiflexion movement of the ankle in stance phase and releases the stored energy in push-off phase. Place of this elastic element is shown in Figure 4.1.5.1.

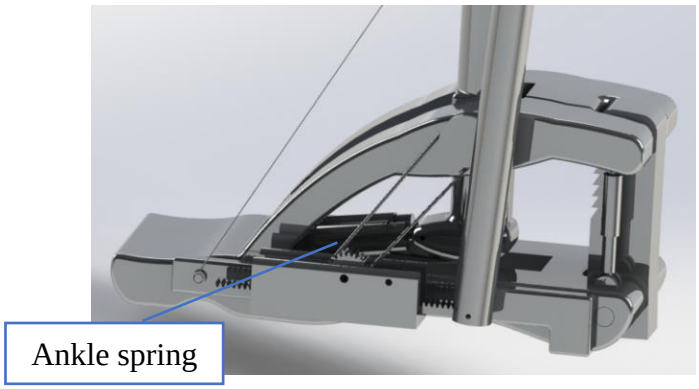

Figure 4.1.5.1 Place of ankle spring

To calculate the coefficient of the ankle spring, dimensions of the prosthesis was used as it is shown in Figure 4.1.5.2.

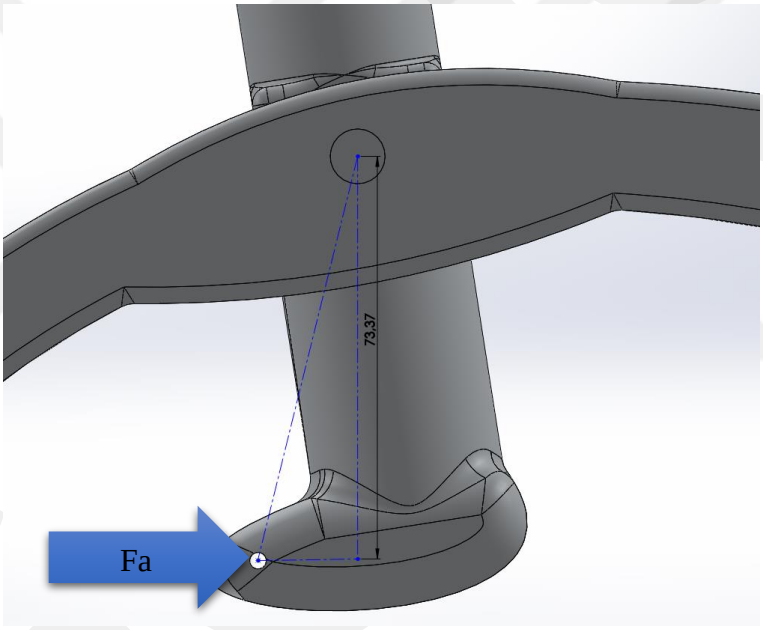

Figure 4.1.5.2 Calculation of the ankle spring

When the shank part of the prosthesis rotates about ankle as 10°, point A moves as 13mm. So, with the help of the distance change and needed force value, spring coefficient of the one ankle spring was calculated as shown in (4.1.5.1) and (4.1.5.2) and so, elastic element behavior was accepted as linear.

$$F_A = \frac{120}{0{,}07337} = 1635{,}54\ N \tag{4.1.5.1}$$

(when the angle at ankle is +10 degrees)

$$k_{ankle\ spring} = \frac{1635{,}54/2}{13} = 62{,}90\ N/mm \tag{4.1.5.2}$$

4.1.6 Coupling Spring

In swing motion of the leg, the foot compartment needs to be raised and here, knee needs to be coupled to the foot-ankle compartment. In other words, knee needs to make flexion movement. For this purpose, the working principle of coupling spring was shown in Figure 3.1.2.1 and Figure 3.1.2.2. The lower connection part of the spring was modified from four rod mechanism to the mechanism as shown in Figure 4.1.6.1. As the lower side of shank rotates about ankle joint wheel rotates too correspondingly, for this purpose, ankle pin is fixed to center of shank, so they rotate together as shown with green arrows. With the help of this mechanism and cable, rack mechanism can be moved about the arrow direction as shown in figure with orange arrows. And elongation of the swing spring can be provided by using this system. In Figure 4.1.6.2, elongation vs force graph of the swing spring is shown.

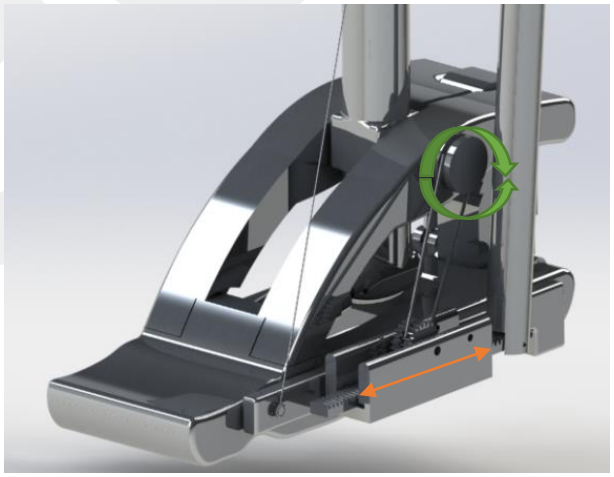

Figure 4.1.6.1 Lower connection joint of swing spring

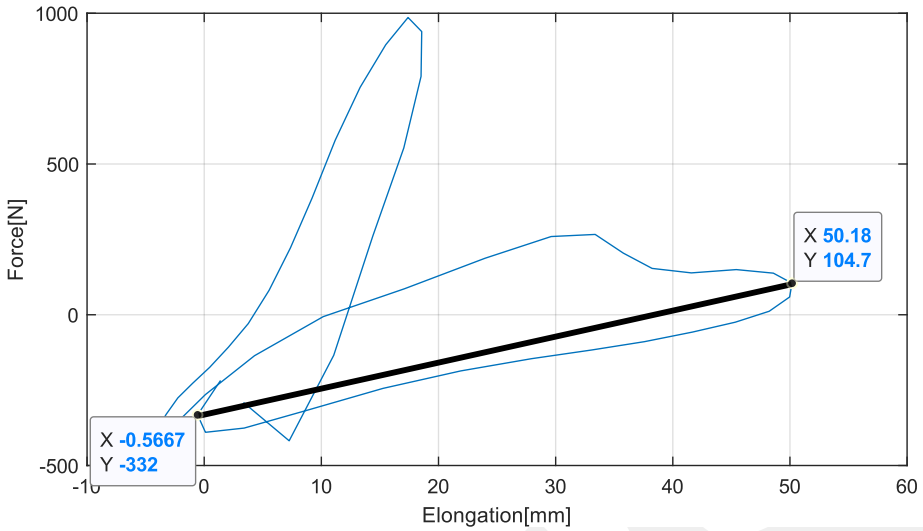

Figure 4.1.6.2 Elongation vs force graph for coupling spring

$$k_{coupling} = \frac{(104{,}7 - (-332)}{50{,}18 - (-0{,}56)} = 8{,}6\ N/mm \qquad (4.1.6.1)$$

4.2 Results

4.2.1 Results and Discussion

The knee joint behavior of the prosthesis and natural knee was compared by using simulation during weight acceptance. Behavior of these knees are shown in Figure 4.2.1.1. As it is seen from figure, their behaviors are similar. So, the WalkMECH 2.1 can nearly mimic the behavior of natural knee.

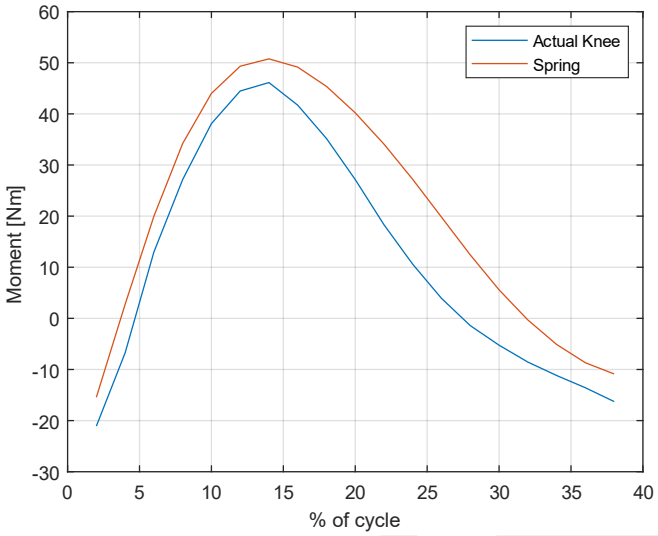

Figure 4.2.1.1 Moment vs gait cycle graph of actual knee and spring for weight acceptance. Actual knee data was adapted from [52].

Similarly, just like the weight acceptance behavior, sit-to-stand behavior of the knee was analyzed by using simulation. And the graph of this simulation is shown in Figure 4.2.1.2. The linear graph shows the behavior of spring and the one with slope shows the behavior of biological knee. The difference of these graphs would be caused by linear approximation as depicted in previous chapter.

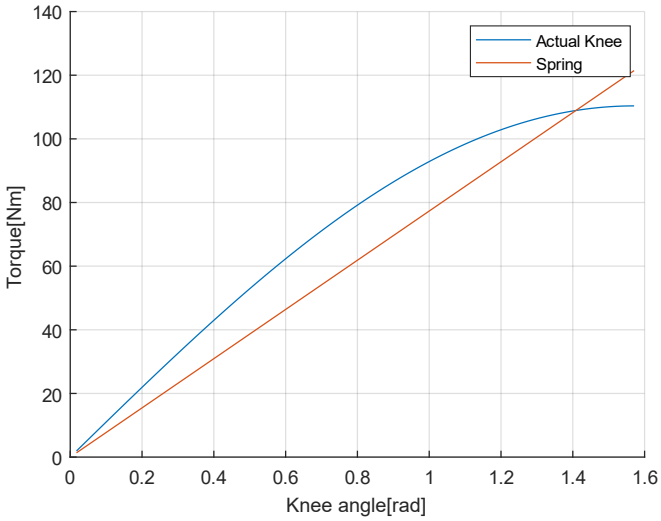

Figure 4.2.1.2 Torque vs angle graph of actual knee and spring during sit to stand

Also torque vs power graphs of the prosthesis and natural knee during stair ascending phase was generated by using simulation as shown in Figure 4.2.1.3. Because the coefficients of the weight acceptance spring and stair climbing springs are close each

other, weight acceptance spring was used for stair climbing task too. Here, the moment of naturel knee starts from 0Nm, but moment of mechanism starts from 40Nm. So, there are 40Nm moment difference between natural knee and the prosthesis and after a while, for further phases the difference decreases. Therefore, spring is compressed with the help of DC motor. At 0% of gait cycle, motor starts to release compressed spring and according to needed moment, actuator set the compression of the spring. Generated graph of power vs walking gait cycle is shown in Figure 4.2.1.3. So, it was observed that with the help of spring, the power need of actuator during first 40% of stair climbing cycle decreased compared to actual knee as 100 W.

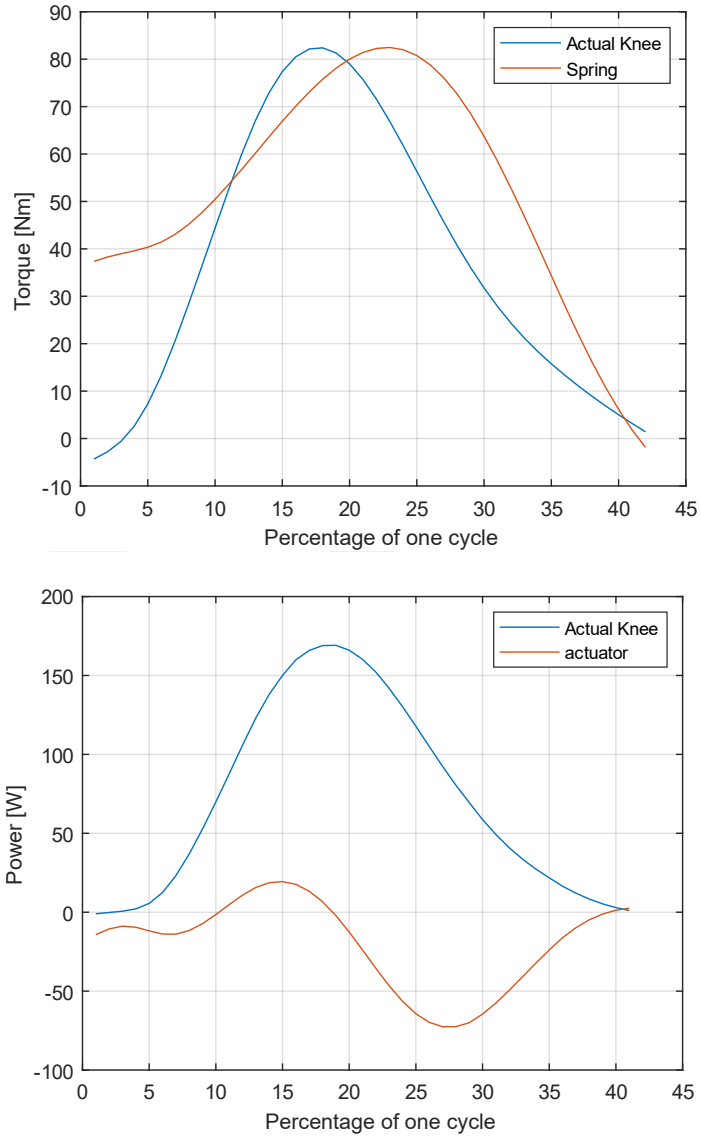

Figure 4.2.1.3 Moment and power plots for stair ascending. In this graph, actual knee data was adapted from [53].

To be able to set the elastic element mechanism, an engage-disengage mechanism was implemented to prosthesis foot compartment as shown in Figure 4.2.1.4. The mechanism starts to engage stair ascending spring with the heel contact of foot and disengages the mechanism with the heel-off. So, the spring is active between 0% and 40% of gait cycle and between 40% and 100% of gait cycle it is deactivated. This is why Figure 4.2.1.3 was plotted between 0% and 40% of the gait cycle.

Figure 4.2.1.4 Engage-disengage mechanism on foot compartment

The knee joint behavior during the forward swing motion for prosthesis and natural knee was compared by using simulation. The figure of this behavior is shown in Figure 4.2.1.5. So, as it seen from figure, the conceptual prosthesis can nearly mimic behavior of natural knee.

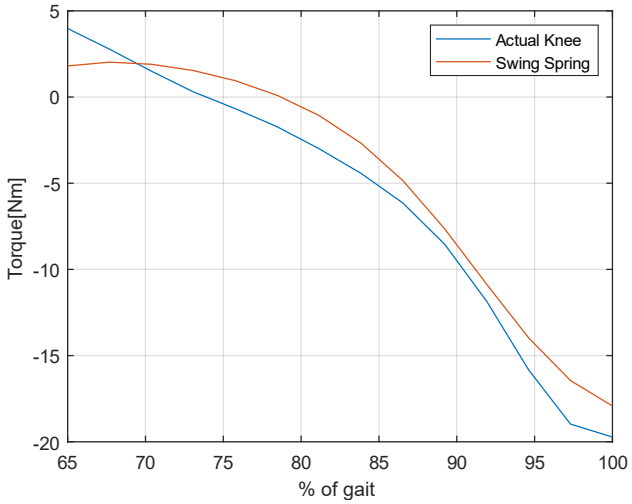

Figure 4.2.1.5 Knee behavior during swing motion. Actual knee data was adapted from [52].

Figure 4.2.1.6 shows the 3D CAD of all parts of WalkMECH 2.1 conceptual prosthesis design. And Figure 4.2.1.7 is the closer look of ankle-foot compartment. The Figure 4.2.1.7 highlights the changes of ankle-knee compartment from WalkMECH2.0 and motion mechanism of coupling elastic element. Upper side of the foot compartment was divided to two pieces as shown in Figure 4.2.1.7, so the ability for walking on different surfaces would be enhanced with the help of bending. Furthermore, places of weight acceptance elastic element, sit-to stand elastic element, stair climbing elastic element were changed to make them more compact and to enhance functionality and they were depicted in title 4.1.1, 4.1.2, 4.1.3 respectively.

Figure 4.2.1.6 3D CAD design of all parts of conceptual design WalkMECH 2.1

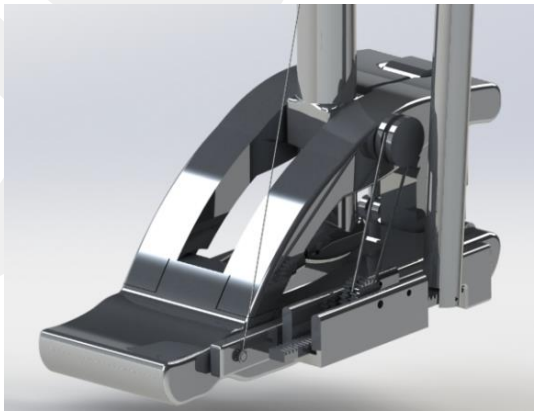

Figure 4.2.1.7 Close-up of ankle-foot compartment

Chapter 5

Topology Optimization of the Prosthesis

In this chapter, design optimization of the foot-ankle compartment, knee compartment and connection part of prosthesis is described. While optimizing the design biomechanical human data were used and as a FEM analysis tool, Ansys Workbench was used. Before starting to optimization, shape of the foot was decided and it was depicted in chapter 3, title 3.2.1.

5.1 Methodology

5.1.1 Topology Optimization Process

Topology optimization can be expressed as optimizing a given part structurally under given constraints by modifying the material distribution [56]. To decrease the weight of the prosthesis and increase the comfort, and usefulness by minimizing the components used for prosthesis, topology optimization was applied on the conceptual design prosthesis. The process of topology optimization for prosthesis is shown in Figure 5.1.1.1. This topology optimization process was applied for the ankle-foot compartment and knee compartment respectively. In this process firstly, initial design was made by using Solidworks. After that, the design was imported as .xt file to Ansys.

Then, conditions for stress analysis were defined in structural analysis tool of Ansys. The results give ideas about the design. After that, according to stress analysis results, topology optimization tool was used for model. In this study, as objective of the optimization process compliance was chosen and as response constraint mass reduction was chosen. With the help this choice, stiffness was kept maximum and at the same time, mass reduction could be assured [57,58].

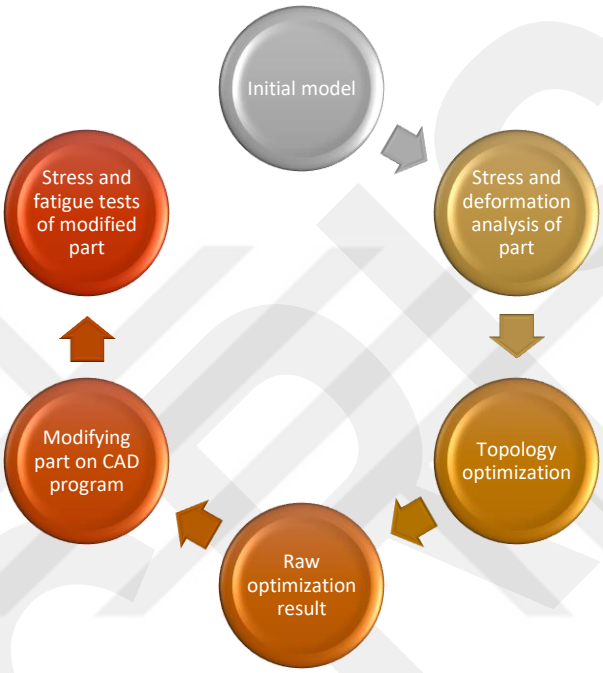

Figure 5.1.1.1 Topology optimization algorithm [59], applied for optimization of prosthesis.

5.1.2 Theoretical Basis of Topology Optimization

The algorithm of the topology optimization in Ansys environment is expressed as follows [58].

$$"f = a\,minimum/maximum\; w * r * t * \eta_i$$

$$0 < \eta_i \leq 1\ (i = 1,2,3 \ldots, N)$$

$$\underline{g_j} < g_j \leq \overline{g_j}\ (j = 1,2,3, \ldots, M)$$

In these equations; f, η_i, N, M, g_j, $\underline{g_j}$, $\overline{g_j}$ respresent the objective function, design variable, number of elements, number of constraints, computed jth constraints value, lower and upper bound for jth constraint value respectively." [58].

In this study, as objective of the topology optimization tool, minimizing the compliance was chosen. In [58], the task of this selection is expressed as maximizing the static stiffness. The algorithm of the process is expressed as follows [58].

$$"U_c = a\ minimum\ w.r.t.\eta_i$$

$$0 < \eta_i \leq 1\ (i = 1,2,3 \dots, N)$$

$$V \leq V_0 - V^*\ \text{(If optimization is subjected to volume constraint)}$$

In these equations; U_c, V, V_0, V^*, V represent the static compliance, computed volume, original volume, amount of material which will be removed respectively." [58].

Used mesh size function in this study is proximity and curvature. Here, curvature size function analyses the rounded sections and calculate the dimensions of meshes [60]. Used proximity size function was based on faces and edges function, this choice increases the number mesh and calculation time, but to have better results, faces and edges choice was chosen for proximity function in Ansys [60].

In this study, used mesh type is tetrahedral type by default.

5.1.3 Optimization of Ankle-Foot Compartment

Stress analysis of foot was made by using FEM analysis method. Ansys workbench tool was used for the FEM analysis. To make the FEM analysis, part was designed in Solidworks. And imported to Ansys workbench as.xt file. Applied material properties is AL 7075-T6 [61]. The analysis was made for the case when the user is at stance phase. Because in this case, the weight on the prosthesis is maximum which is equal to 784,8 N (80kg*9,81m/s^2). On the other hand, previous studies on structure of the foot was depicted in title 3.2.1. Here, topology optimization of the part will be depicted.

Before the solution is applied, the mesh properties were defined as shown in Figure 5.1.3.1. Total number of nodes for this part is 279637 and total number of elements for this part is 183083.

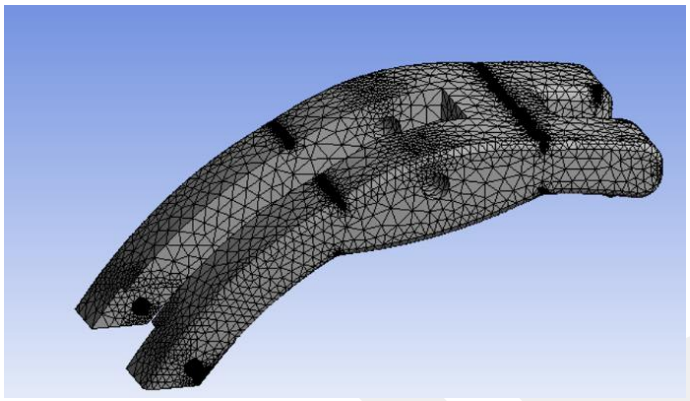

Figure 5.1.3.1 Mesh distribution of upper side of foot

Stress result of the upper side of foot is shown in Figure 5.1.3.2.

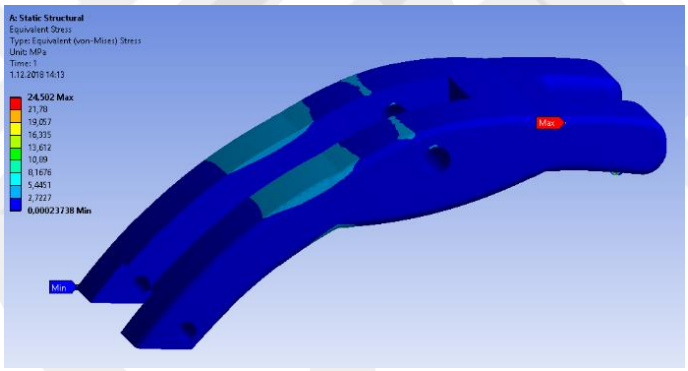

Figure 5.1.3.2 Stress results of applied FEM analysis

Deformation result of the upper side of foot is shown in Figure 5.1.3.3

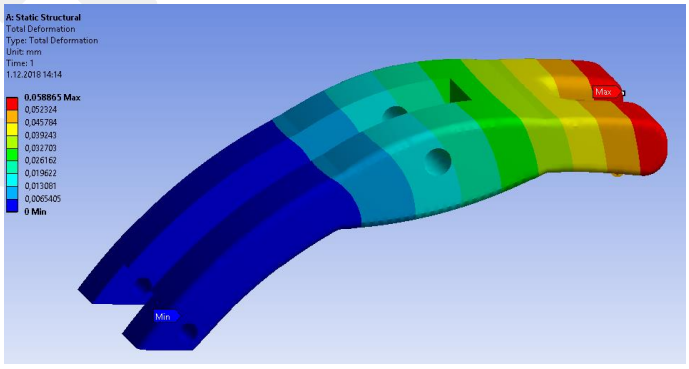

Figure 5.1.3.3 Deformation result of the part

Strain analysis result of the part is shown in Figure 5.1.3.4.

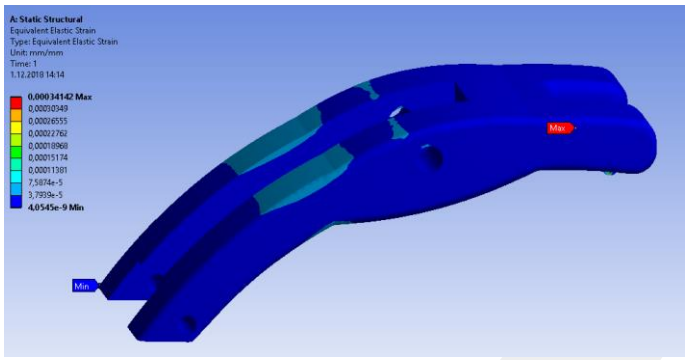

Figure 5.1.3.4 Strain result of the part

According to structural stress analysis results, areas with blue color represents the low stress areas. So, the mass of the upper side of foot compartment can be decreased by means of topology optimization method. For this purpose, topology optimization tool of Ansys Workbench was used. Here, percent of retain mass was applied as 60% and objective of this optimization process was minimizing the compliance. Totally 21 iteration was made. On Figure 5.1.3.5, optimization result is seen.

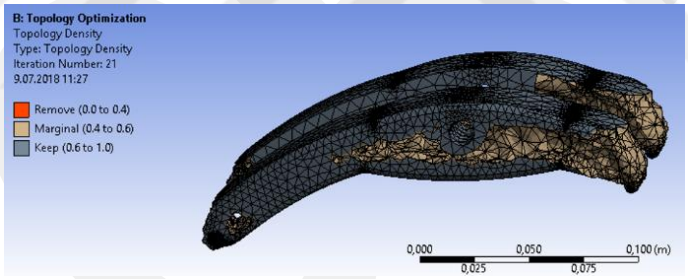

Figure 5.1.3.5 First optimization result of upper side of foot compartment

By taking into account stress result which is shown in Figure 5.1.3.2 and optimization result which is in Figure 5.1.3.5, it has been observed that the foot design needs to be modified to make it light and compact. So, to do that, the design was modified as shown in Figure 5.1.3.6. The width and thickness of foot compartment was decreased also. Total volume of the part was decreased from 420 cm^3 to 161 cm^3.

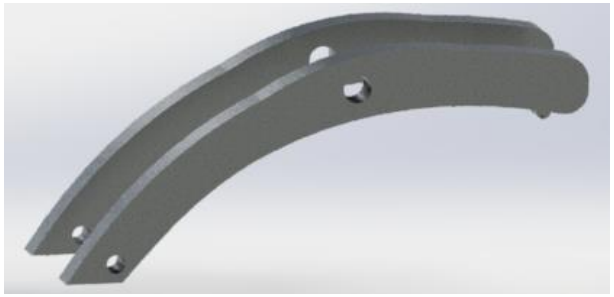

Figure 5.1.3.6 Modified foot compartment

Following that the modified part was analyzed in Ansys environment again. And the same forces of initial model were applied on this part. Total number of nodes is 176802 and total number of elements is 115586 for this analysis. The stress result of this part is shown in Figure 5.1.3.7. It is clear that stress distribution of modified part is more regular compared to Figure 5.1.3.2 which is the stress result of the unmodified part. However, to decrease the weight and to make finer design, modified part was put into topology optimization process again. Topology optimization result of the modified part is shown in Figure 5.1.3.10. In this process, totally 35 iterations were performed.

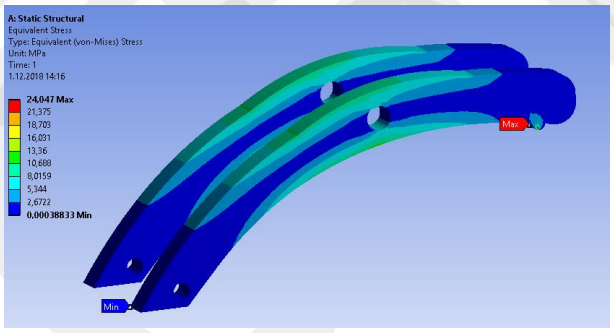

Figure 5.1.3.7 Stress result of modified part

Deformation result of the upper side of foot is shown in Figure 5.1.3.8

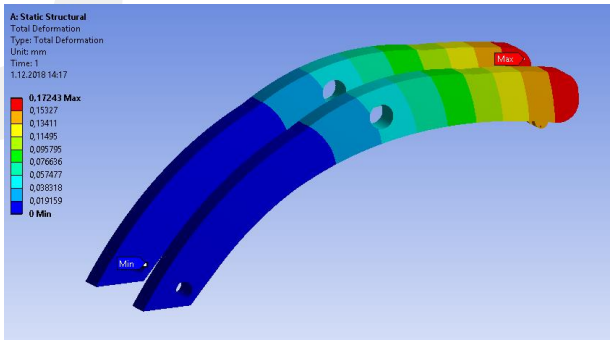

Figure 5.1.3.8 Deformation result of the upper side of foot

Strain result of the upper side of foot is shown in Figure 5.1.3.9.

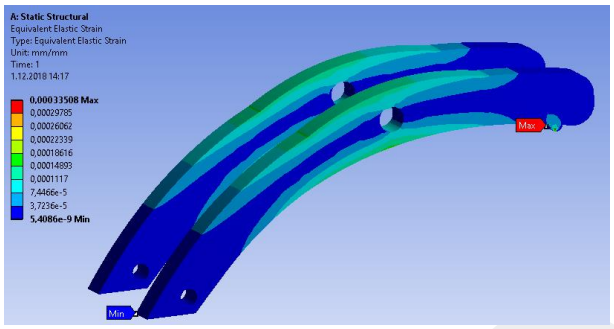

Figure 5.1.3.9 Strain result of the upper side of foot

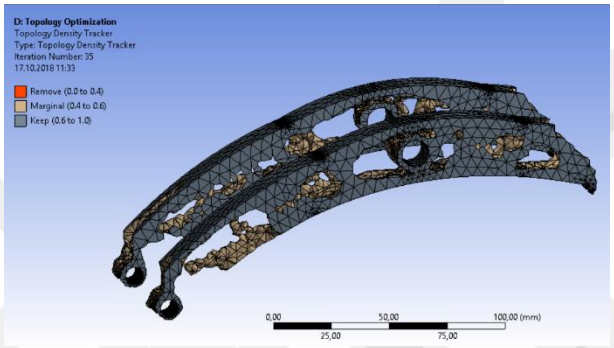

Figure 5.1.3.10 Topology optimization result of modified part

The part was modified considering the topology optimization result that is in Figure 5.1.3.10. And the topology optimization result was exported as .stl file and it was matched with modified part by using solidworks as shown in Figure 5.1.3.11 to make a finer design and see the removable areas on part.

Figure 5.1.3.11 Matching the modified and raw parts

After matching the parts as in Figure 5.1.3.11, the upper side of foot was modified according to topology optimization result. And the finally the upper side of foot was modified as shown in Figure 5.1.3.12.

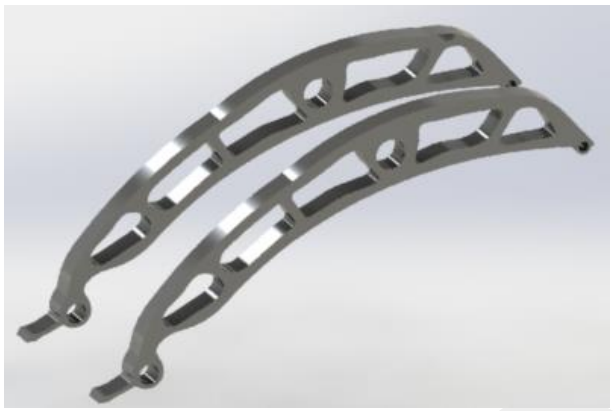

Figure 5.1.3.12 Modified upper side of foot

The modified part analyzed structurally by using Ansys workbench tool. Mesh properties of the part is shown in Figure 5.1.3.13. Number of nodes is 344749 and number of elements is 223243. And the stress result of the upper side of foot is shown in Figure 5.1.3.14.

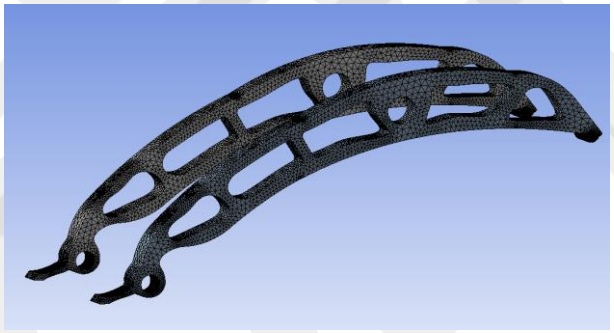

Figure 5.1.3.13 Mesh distribution of the modified upper side of foot

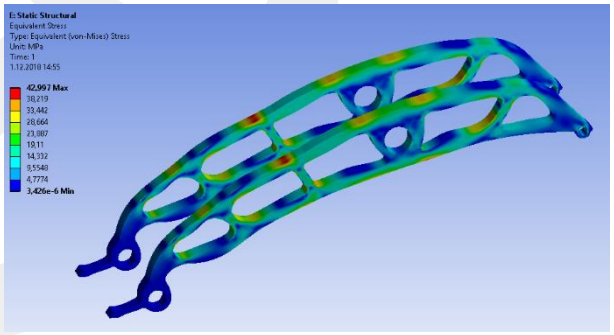

Figure 5.1.3.14 Stress analysis result of modified part

Deformation analysis result of the modified upper side of foot is shown in Figure 5.1.3.15.

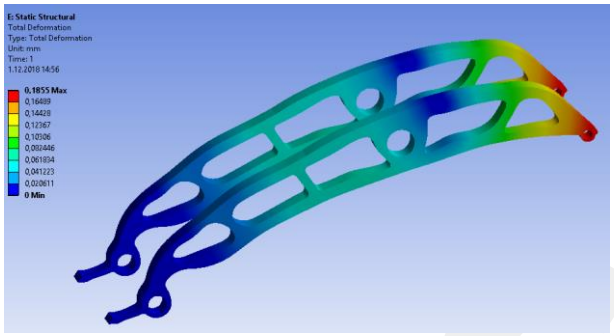

Figure 5.1.3.15 Deformation analysis result of the modified upper side of foot

Strain analysis result of the modified upper side of foot is shown in Figure 5.1.3.16.

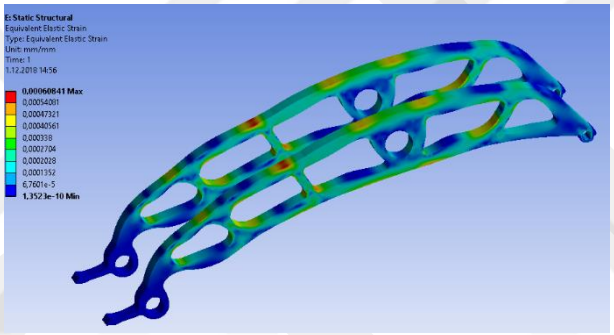

Figure 5.1.3.16 Strain analysis result of the modified upper side of foot part

After analyzing the modified part as shown in Figure 5.1.3.14, Figure 5.1.3.15, Figure 5.1.3.16 just to examine what if connection parts of upper side of foot was removed. This case has been tested that as shown in Figure 5.1.3.17. It has been seen that the connection parts of upper side of foot are necessary by considering stress results as it was expected from Figure 5.1.3.10.

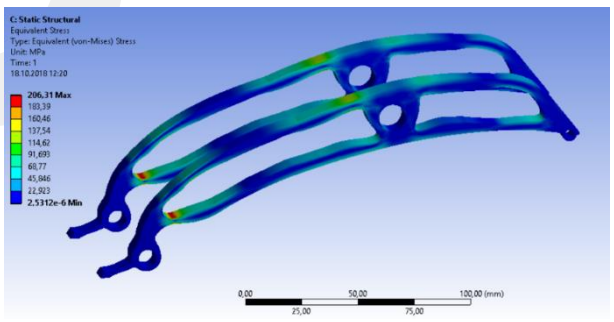

Figure 5.1.3.17 Stress result of the part

5.1.4 Optimization of the Knee Compartment

Initial design of the knee compartment is shown in Figure 5.1.4.1. Before the optimization of knee compartment, the knee was analyzed by using Ansys workbench tool. In this process, firstly the knee design was imported as .xt file format to Ansys Workbench and mesh step of the process is shown in Figure 5.1.4.2. Here, total number of nodes is 32835 and total number of elements is 21309. The material that is used for the knee compartment is AL 7075 – T6 [61].

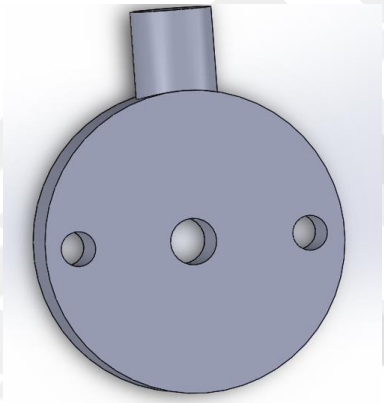

Figure 5.1.4.1 Initial knee design

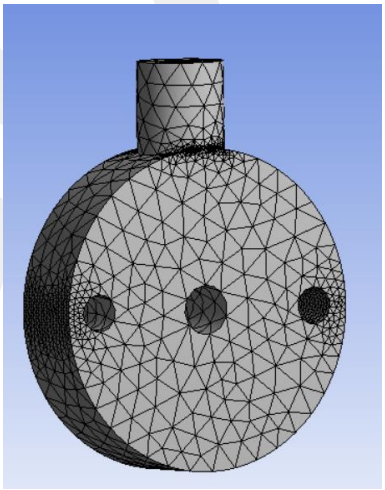

Figure 5.1.4.2 Mesh distribution of the part

Before applying the stress analysis, joints of the knee compartment were defined as shown in Figure 5.1.4.3. In this figure weight acceptance / stair climbing joint, knee joint and coupling spring were shown respectively. For these joints, maximum forces were taken into account. Also, it was accepted that the forces are maximum at the same time, since this approach simplifies the problem because it makes the problem static, also the safety factor will be increased with this approach.

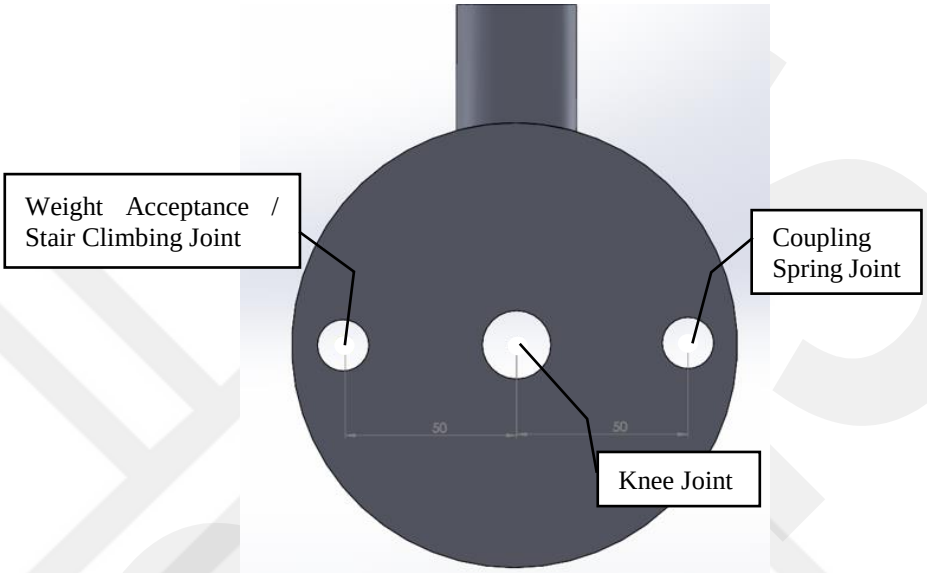

Figure 5.1.4.3 Joint on knee compartment

After defining the problem in Ansys workbench tool, the result of stress analysis of knee compartment is shown in Figure 5.1.4.4.

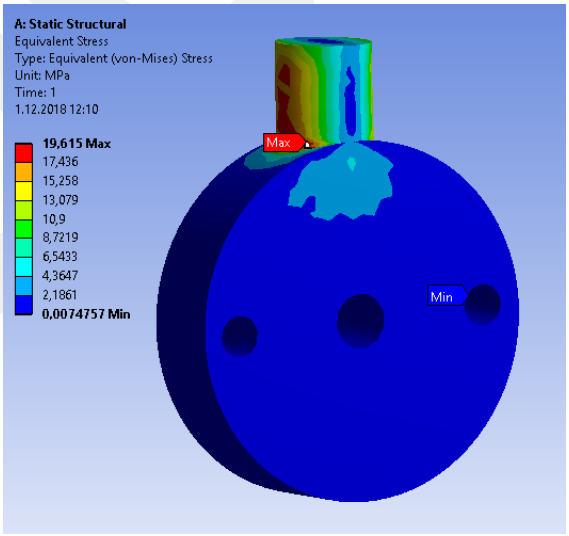

Figure 5.1.4.4 Stress results of knee compartment.

Deformation analysis result of the initial knee compartment is shown in Figure 5.1.4.5.

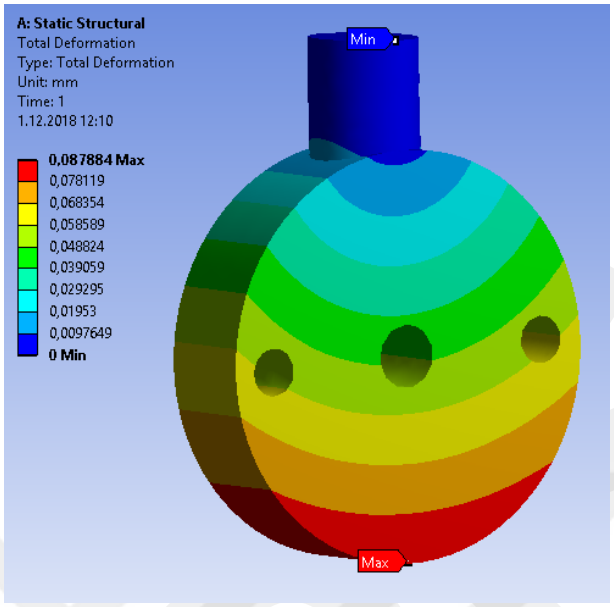

Figure 5.1.4.5 Deformation analysis result of initial model.

Stain analysis result of the initial model of the knee compartment is shown in Figure 5.1.4.6.

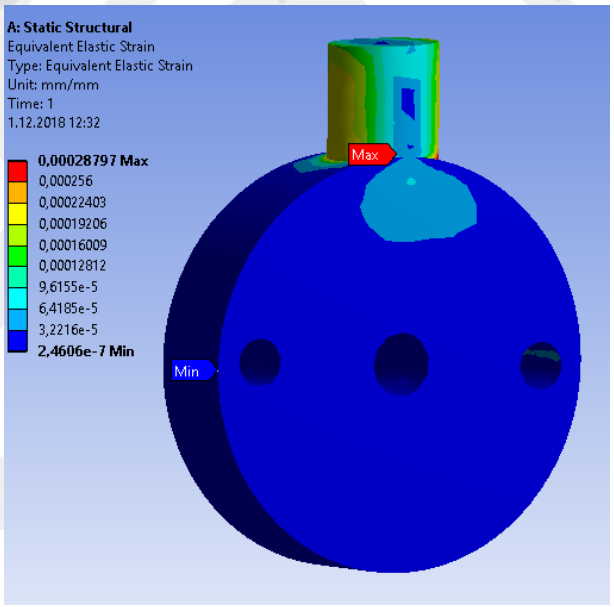

Figure 5.1.4.6 Strain analysis result of the initial model.

As it is seen from Figure 5.1.4.4, blue areas that represents the low stress regions can be modified. So, for this purpose, topology optimization tool of Ansys Workbench

was used. And in this process totally 26 iterations were performed as shown in Figure 5.1.4.7.

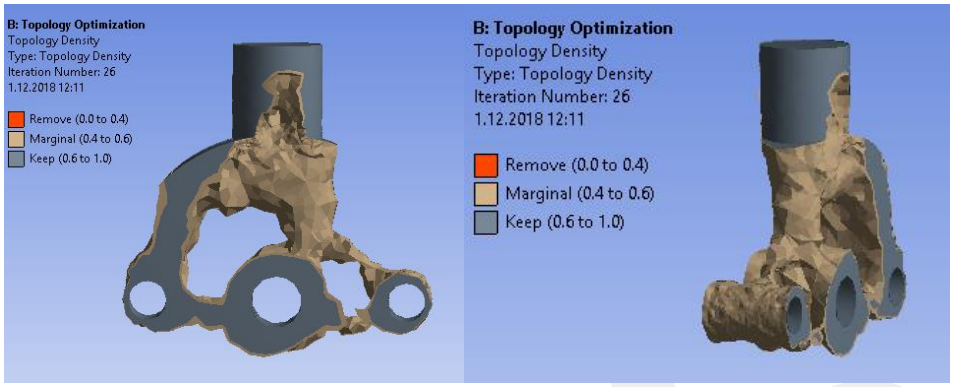

Figure 5.1.4.7 Topology optimization result of optimization process

As it seen from Figure 5.1.4.7, the knee compartment can be modified by using topology optimization result to make the knee compartment lighter and more compact. So, as shown in Figure 5.1.4.8, the topology optimization result was exported from Ansys as .stl file and imported to Solidworks and matched with the initial knee design. And the initial knee design was modified according to topology optimization result.

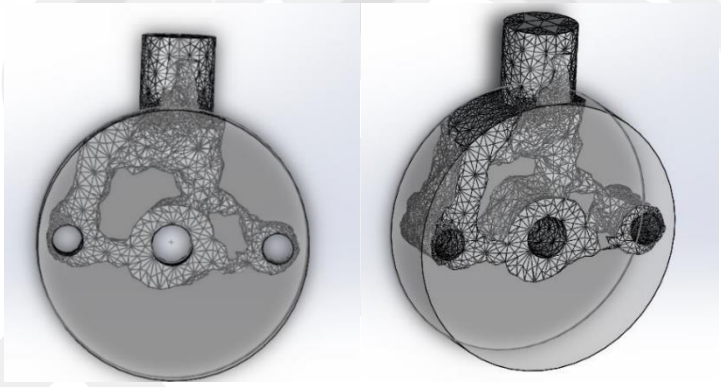

Figure 5.1.4.8 Matching the initial design and optimization result of initial design

At the end of modifying part of topology optimization process, the weight was decreased and part became finer as it is shown in Figure 5.1.4.9.

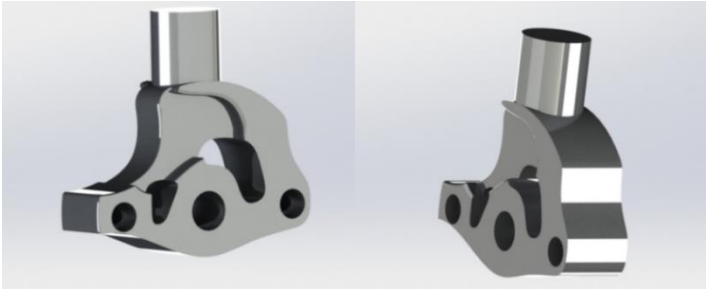

Figure 5.1.4.9 Modified Knee compartment

The modified knee compartment needs to be validated by using Ansys workbench tool so, for this purpose, the part was exported as .xt file format and imported to Ansys environment. AL 7075–T6, was configured for analysis [61] and mesh was applied as it is shown in Figure 5.1.4.10. Here, total number of nodes is 113795 and total number of elements is 74825.

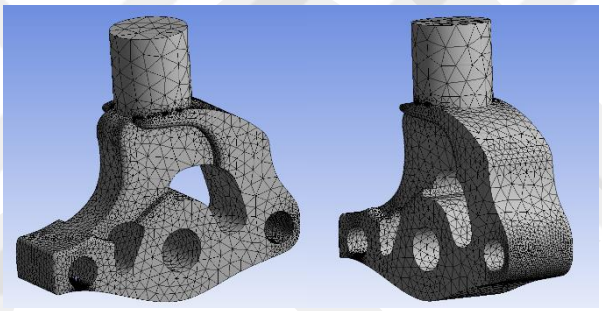

Figure 5.1.4.10 Mesh distribution of knee

The force on this part is applied like Figure 5.1.4.3, so under the same conditions with the initial knee design, the modified part was modeled in Ansys. At the end of this process stress result of the knee compartment part is shown in Figure 5.1.4.11.

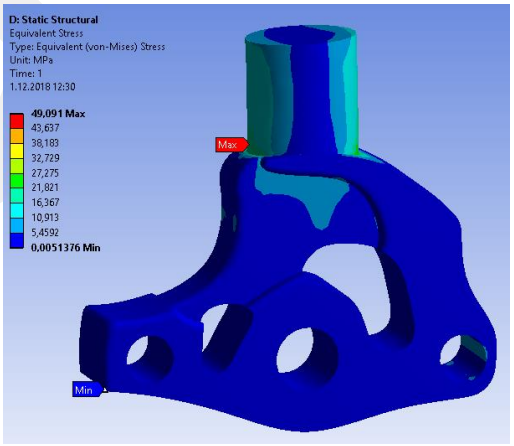

Figure 5.1.4.11 Stress distribution of the modified part

By considering the stress result of modified knee compartment as it is shown in Figure 5.1.4.11, the stress distribution of the modified knee is more regular compared to that of the initial model of the knee compartment.

Deformation analysis result of the modified knee compartment is shown in Figure 5.1.4.12.

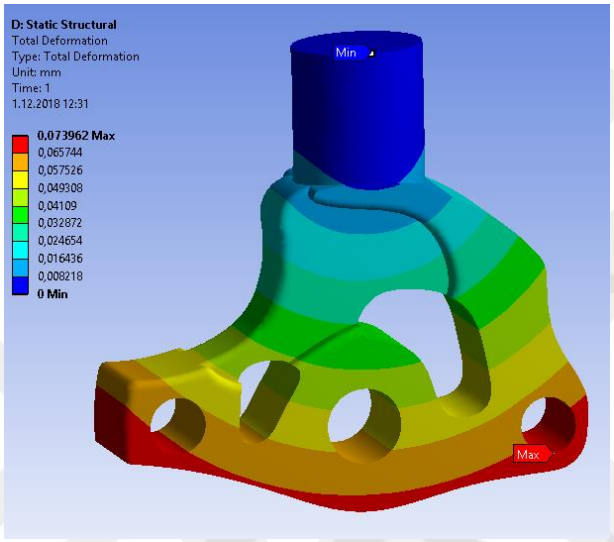

Figure 5.1.4.12 Deformation analysis result of the modified knee compartment

Strain analysis result of the modified knee compartment is shown in Figure 5.1.4.13.

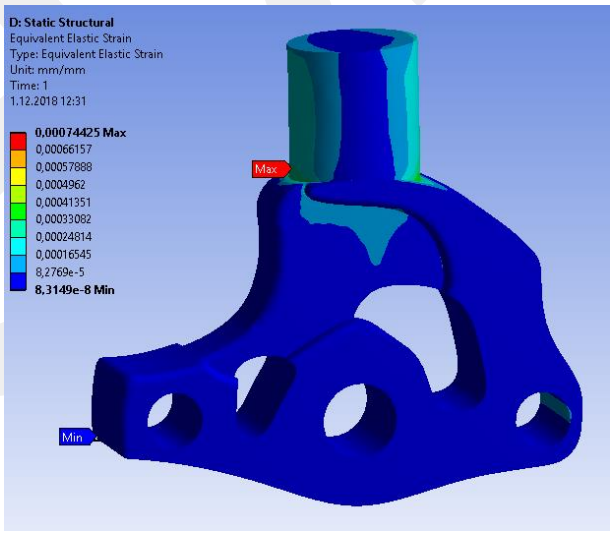

Figure 5.1.4.13 Strain analysis result of the modified knee compartment

5.1.5 Optimization of the Shank Section

For the optimization of shank section of the design firstly maximum forces on parts were calculated with the help of Figure 5.1.5.1 and aqn (5.1.5.1).

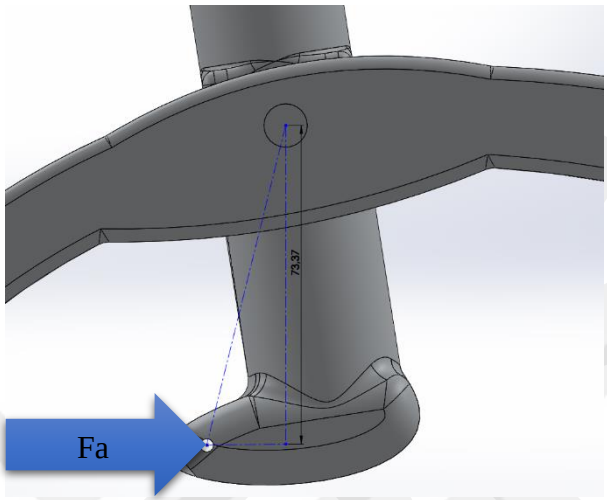

Figure 5.1.5.1 Calculations of maximum forces on lower part of shank.

$$F_A = -\frac{120}{0{,}07337} = -1635{,}54\ N \tag{5.1.5.1}$$

(when the angle at ankle is +10 degrees)

After calculating the forces on the part, the AL 7075-T6 [61] material properties were defined in Ansys. Also applied forces on the part is shown in Figure 5.1.5.2.

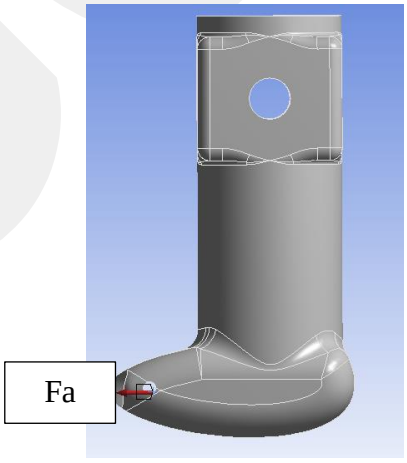

Figure 5.1.5.2 Applied force and joint in Ansys

Mesh distribution of the part was defined as Figure 5.1.5.3. Here, total number of nodes is 201937 and total number of elements is 132557.

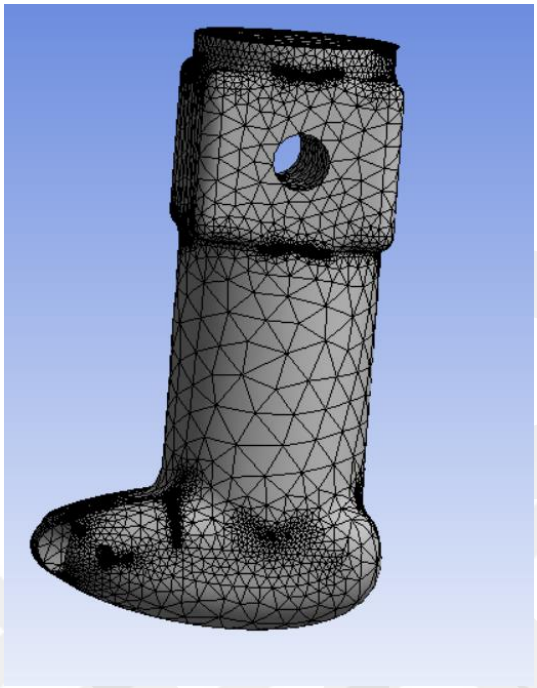

Figure 5.1.5.3 Mesh distribution of the shank part

Total number of nodes is 308647 and total number of elements is 203639 for lower part of shank. After applying the mesh, stress test of the initial shank part was made and the stress result is shown in Figure 5.1.5.4.

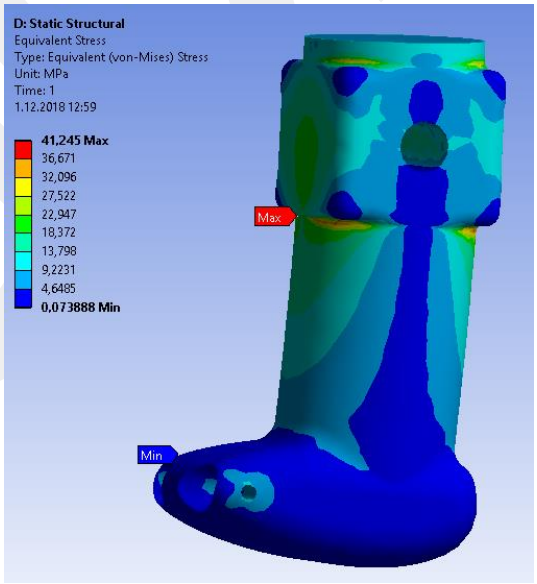

Figure 5.1.5.4 Stress result of the part

Deformation analysis result of the initial model of the shank section is shown in Figure 5.1.5.5.

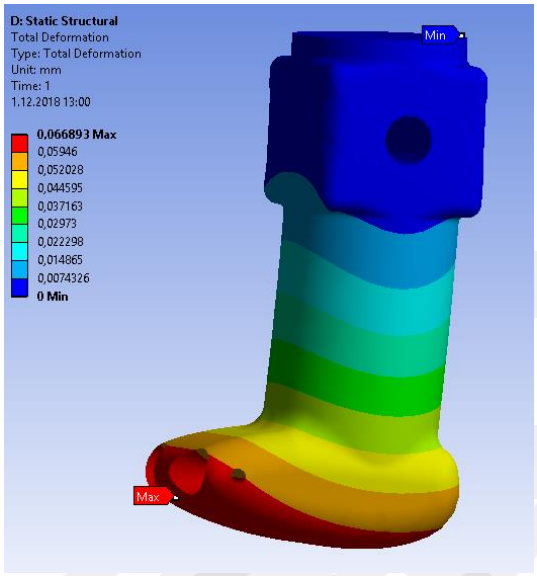

Figure 5.1.5.5 Deformation result of the shank section

Strain analysis result of the initial shank section is shown in Figure 5.1.5.6.

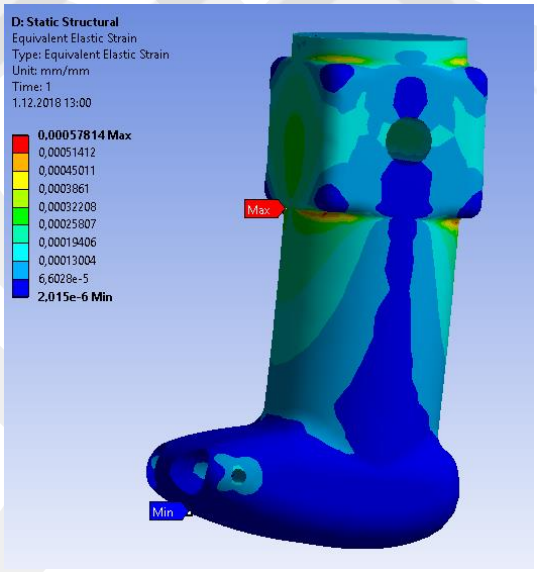

Figure 5.1.5.6 Strain analysis result of the initial shank section.

By considering the stress result of shank section, it can be concluded that the stress distribution on shank part is nearly regular but to decrease the weight, topology optimization for this part was applied and totally 30 iterations were performed as shown in Figure 5.1.5.7.

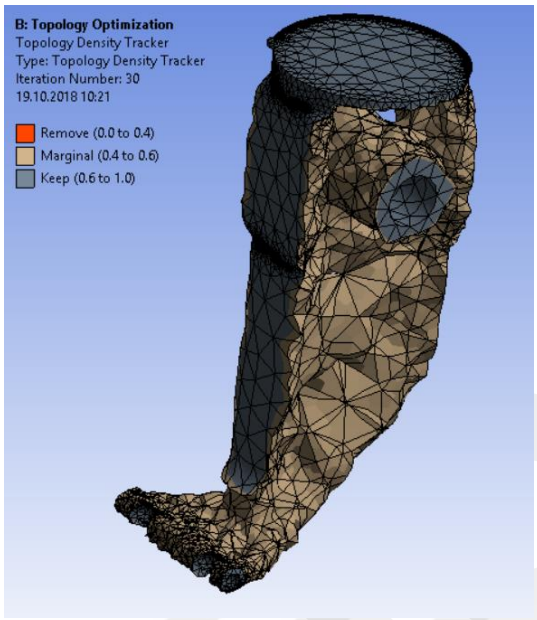

Figure 5.1.5.7 Topology optimization result of the shank section part

According to topology optimization result, the initial part was modified. To do that, the part was exported as .stl file from Ansys and imported to Solidworks environment and the parts were matched in assembly file as shown in Figure 5.1.5.8. In this process the initial part was modified by using topology optimization raw result.

Figure 5.1.5.8 Modifying the shank part in Solidworks

At the end of modification process, the shank became finer and the weight of the shank section was decreased. The optimized shank section needs to be analyzed in terms of stress, so, for this purpose, stress analysis was needed to be performed for shank section.

Figure 5.1.5.9 Modified part

After modifying the shank section part in CAD program, modified shank was imported to Ansys environment and mesh properties of the shank is shown in Figure 5.1.5.10. Here, the number of the nodes is 419068 and the number of the elements is 279197.

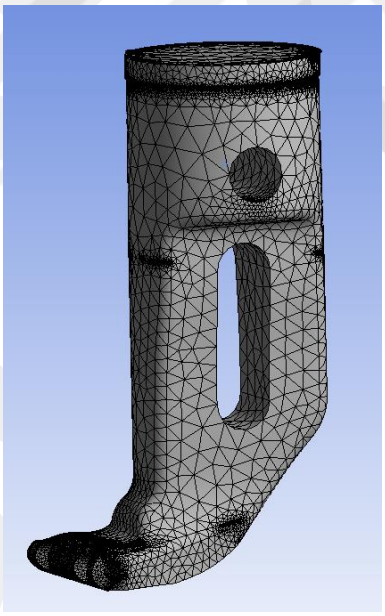

Figure 5.1.5.10 Mesh distribution of the modified shank section.

Stress analysis of the shank section part is shown in Figure 5.1.5.11.

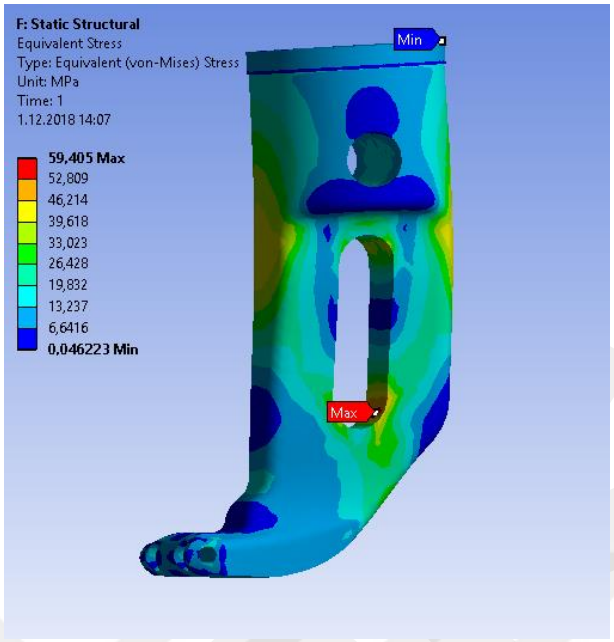

Figure 5.1.5.11 Stress result of the shank section

Deformation analysis result of the shank part is shown in Figure 5.1.5.12.

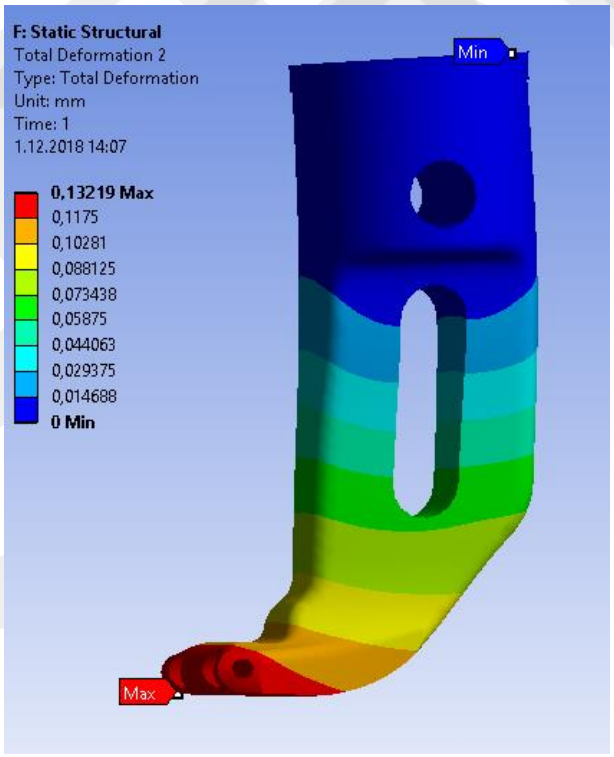

Figure 5.1.5.12 Deformation analysis result of the shank section.

The strain result of the modified shank section is shown in Figure 5.1.5.13.

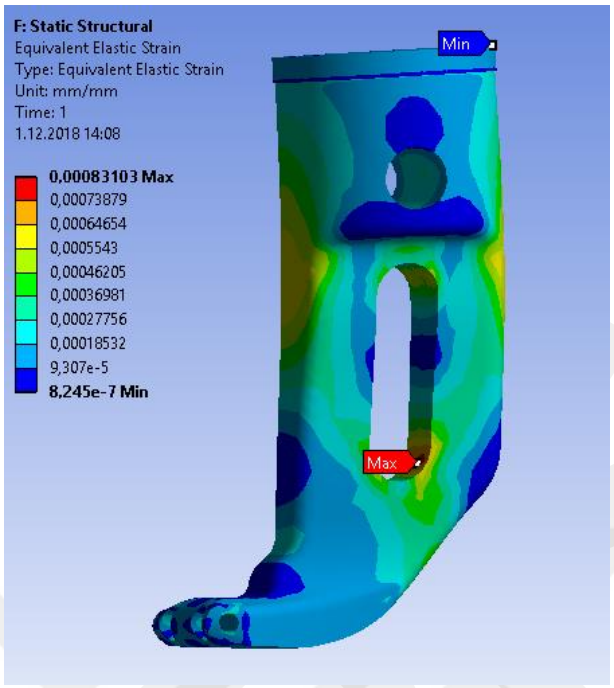

Figure 5.1.5.13 Strain result of the modified shank part.

5.1.6 Optimization of the Connection Part of Elastic Element in Shank Section and Knee

The connection part between the elastic element in shank and knee compartment is shown in Figure 5.1.6.1. The maximum load on this part is applied during stair ascending task, so the part was analyzed under the condition of stair climbing. The applied material properties is AL 7075-T6 [61]. Mesh properties of the part is seen in Figure 5.1.6.2. The number of nodes for the part is 34157 and the number of the elements is 21752 for this part.

Figure 5.1.6.1 Connection part

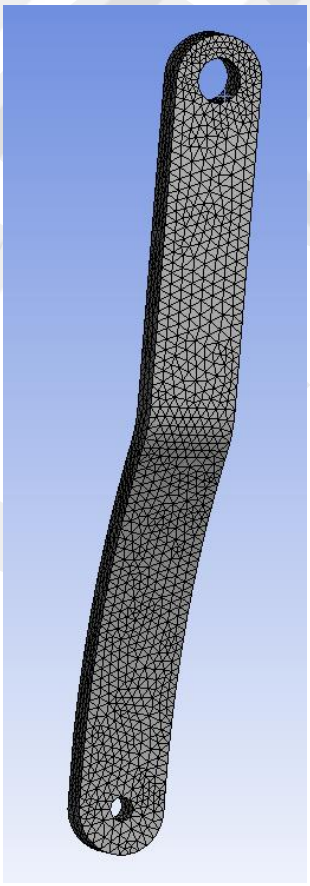

Figure 5.1.6.2 Mesh properties of the initial connection part.

The stress, deformation and strain analysis results of the connection part are shown in Figure 5.1.6.3, Figure 5.1.6.4, Figure 5.1.6.5 respectively.

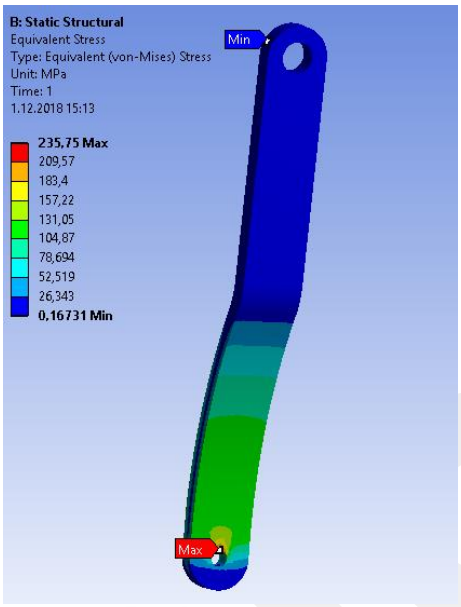

Figure 5.1.6.3 Stress analysis result of the initial connection part.

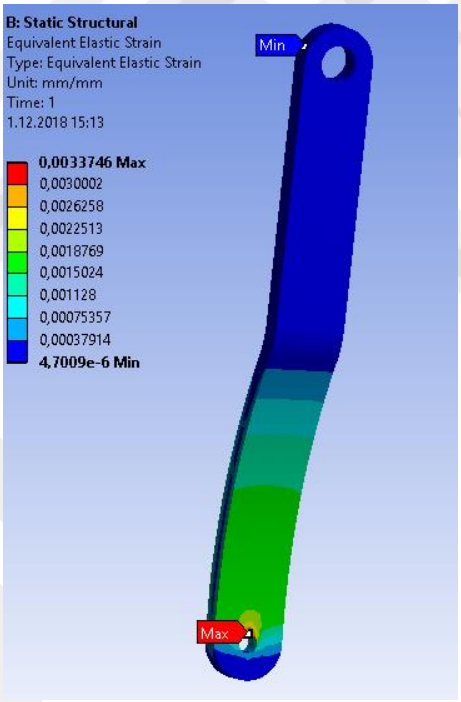

Figure 5.1.6.4 Strain analysis result of the initial connection part.

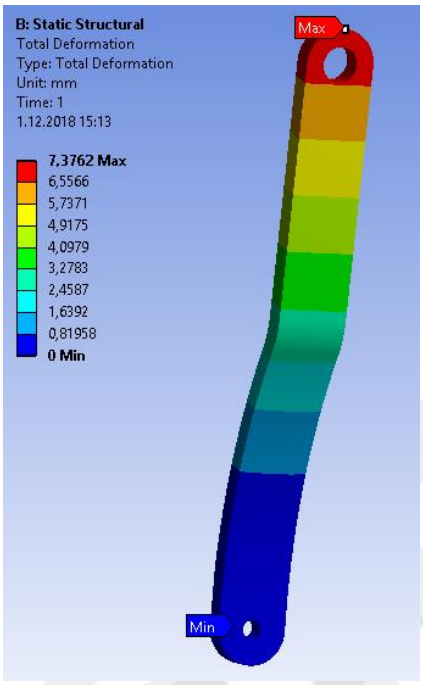

Figure 5.1.6.5 Deformation analysis result of the initial connection part.

It is clear that, according to actual shape of the connection part, curvature part would be problematic to be sure about that, life and safety factor of the part were analyzed by using FEM analysis method. In Figure 5.1.6.6, Figure 5.1.6.7 safety factor and life values of the parts are shown respectively.

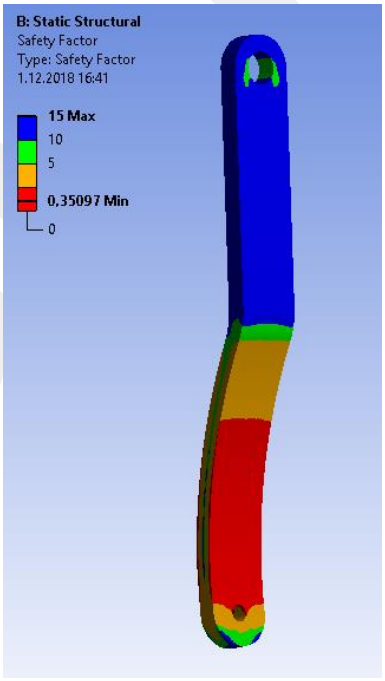

Figure 5.1.6.6 Safety factor of the initial connection part

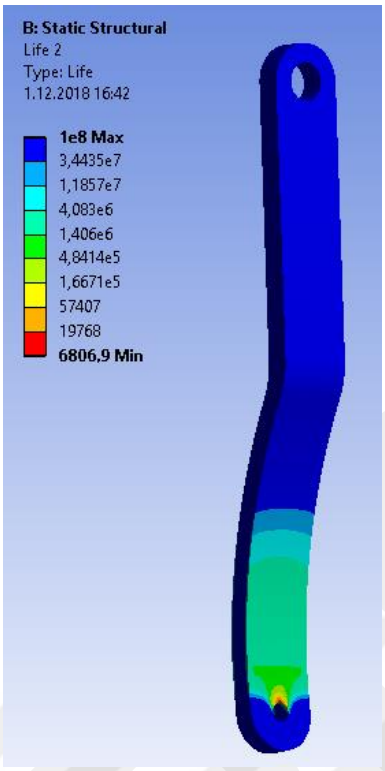

Figure 5.1.6.7 Life of the initial connection model.

As it is seen from Figure 5.1.6.6 and Figure 5.1.6.7 the minimum safety factor of the part is very low. Because of this reason, the part was redesigned and the thickness at lower side of part was increased as shown in Figure 5.1.6.8. And the same analysis was repeated again.

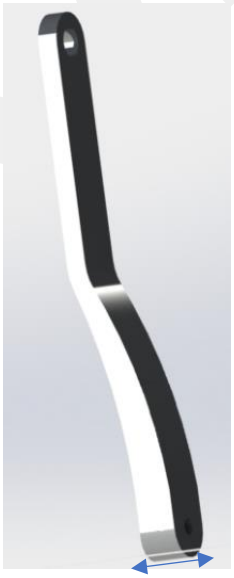

Figure 5.1.6.8 Modifying the initial part

For the FEM analysis of the modified part, the number of nodes was 24550 and number of elements was 15532. Under same conditions with initial part, analysis was made.

Stress analysis of the modified part is shown in Figure 5.1.6.9.

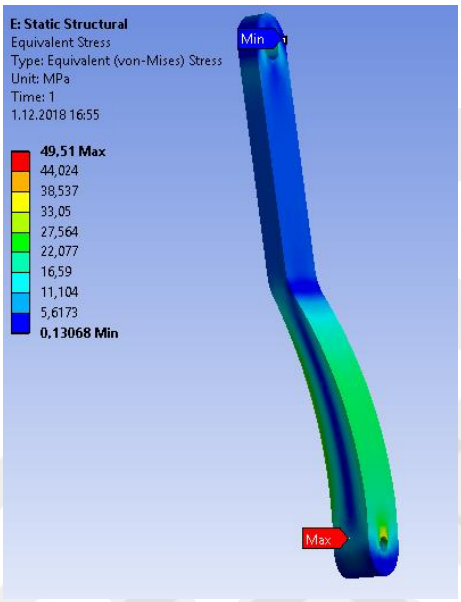

Figure 5.1.6.9 Stress result of the modified connection part.

Deformation analysis of the modified connection part is shown in Figure 5.1.6.10

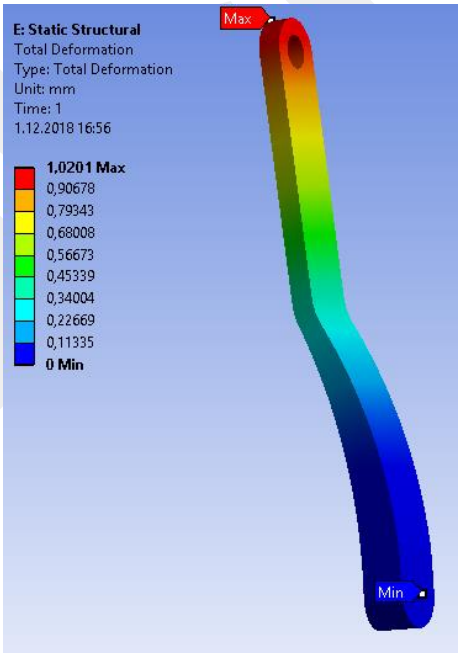

Figure 5.1.6.10 Deformation analysis result of the modified connection part.

Strain analysis of the modified connection part is shown in Figure 5.1.6.11.

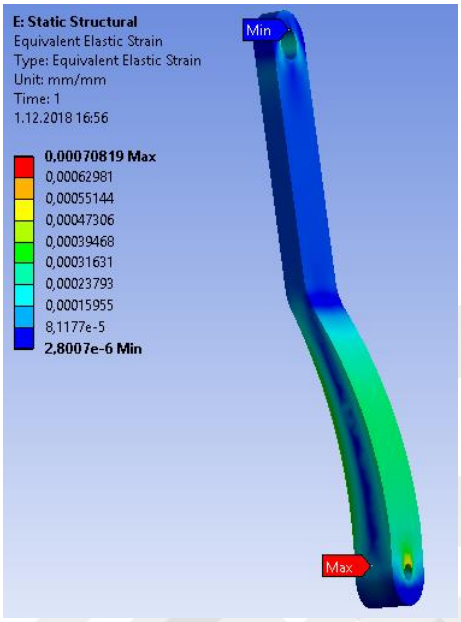

Figure 5.1.6.11 Strain analysis result of the modified connection part.

Fatigue analysis of the modified connection part was made and life and safety factor of the modified part are shown in Figure 5.1.6.12 and Figure 5.1.6.13.

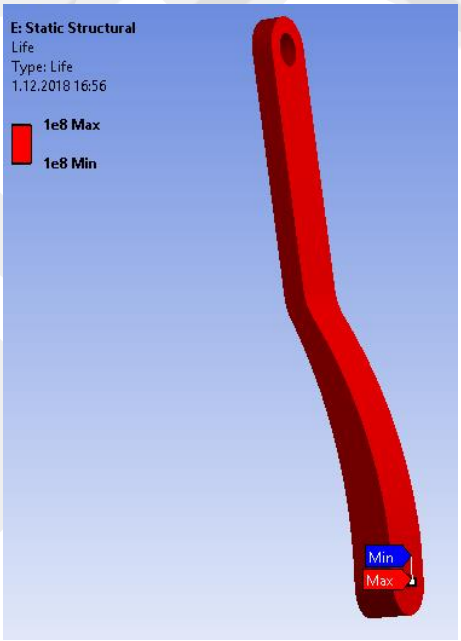

Figure 5.1.6.12 Life analysis result of the modified connection part.

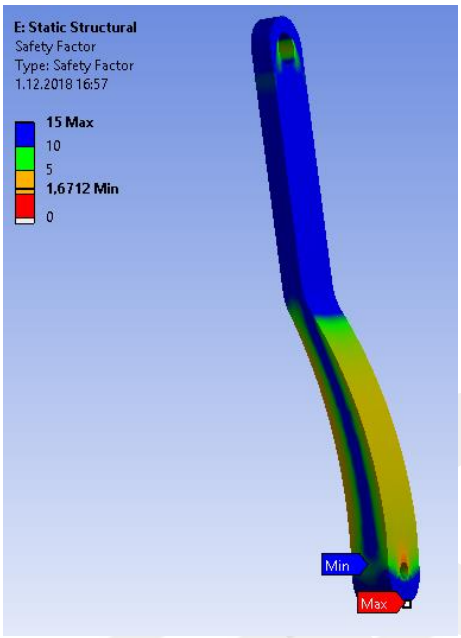

Figure 5.1.6.13 Safety factor analysis result of modified connection part.

It is clear with the safety factor and stress test results, the part is safe, but according to stress analysis results, the part can be lightened, so topology optimization was made as shown in Figure 5.1.6.14. Here, totally 44 iterations were made.

Figure 5.1.6.14 Topology optimization of the modified connection part.

The topology optimization result was exported from FEM program and imported to CAD program and modified there. The process of this step is shown in Figure 5.1.6.15.

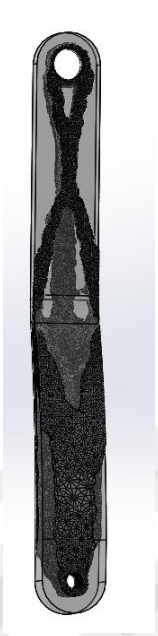

Figure 5.1.6.15 Modifying the connection part in CAD program

Thereafter, modified part was imported to Ansys environment and under the same conditions with the initial connection part, analyzed structurally. Mesh properties of the part is shown in Figure 5.1.6.16. For this step, total number of nodes for this part is 73471 and number of elements is 48070.

Figure 5.1.6.16 Mesh of the modified connection part.

Stress result, deformation and strain result of the modified connection part are given in Figure 5.1.6.17, Figure 5.1.6.18 and Figure 5.1.6.19 respectively.

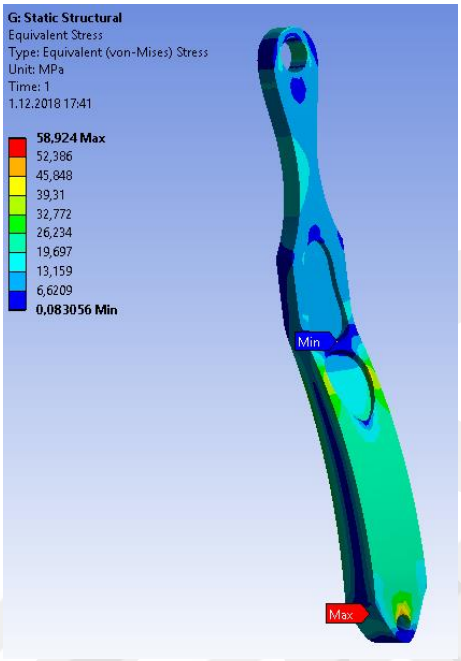

Figure 5.1.6.17 Stress analysis result of the optimized connection part.

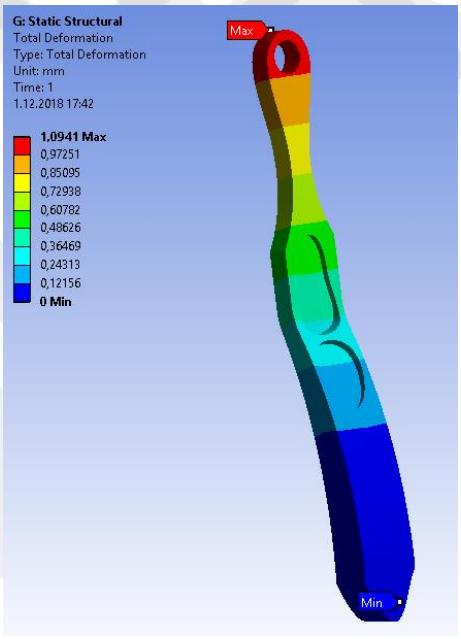

Figure 5.1.6.18 Deformation analysis result of the optimized connection part.

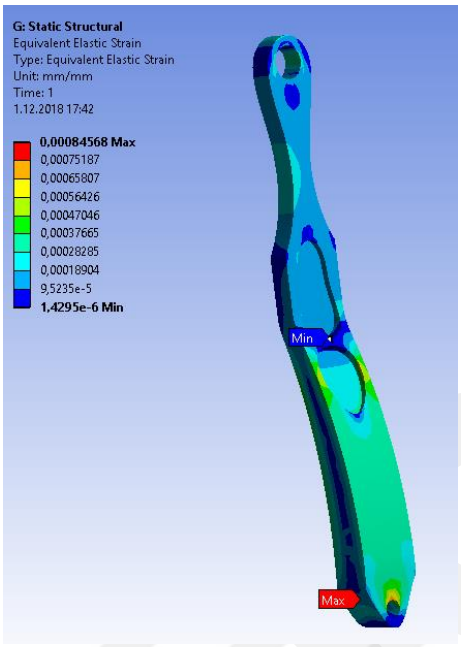

Figure 5.1.6.19 Strain analysis result of the optimized connection part.

5.2 Results

5.2.1 Results and Discussion

In this chapter optimization of the ankle, knee, shank section and also connection parts in terms of structural is described. To decrease the weight and also increase compactness, topology optimization process was applied. And, topology optimization process, mass-based optimization was applied. In this type of topology optimization, percent of retain mass was applied as 30% and objective of this optimization process was minimizing the compliance which helps to keep maximum the stiffness [57,58]. And according to optimization results 'percent of retain' value was configured in terms of observing the most important trajectories in structure.

After modified parts were analyzed in stress tool of Ansys, the parts were analyzed in terms of safety, under same conditions. And life cycles of parts were analyzed to see fatigue life of parts. The results of this step are shown in Figure 5.2.1.1, Figure 5.2.1.2, Figure 5.2.1.3, Figure 5.2.1.4, Figure 5.2.1.5 and Figure 5.2.1.6.

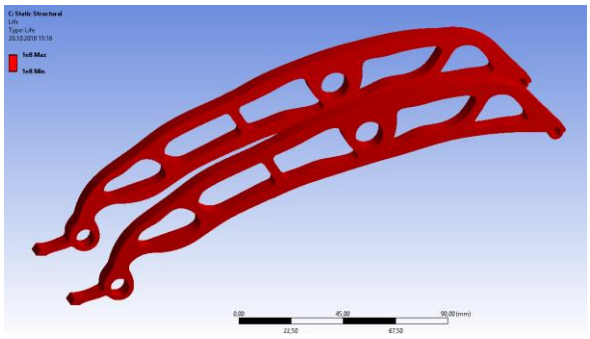

Figure 5.2.1.1 Life analysis result of modified upper side of foot compartment

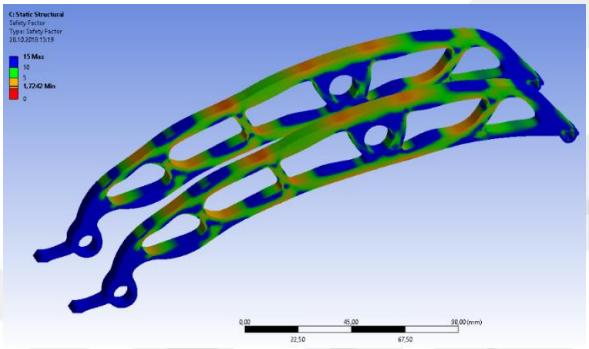

Figure 5.2.1.2 Safety factor result of modified upper side of foot compartment

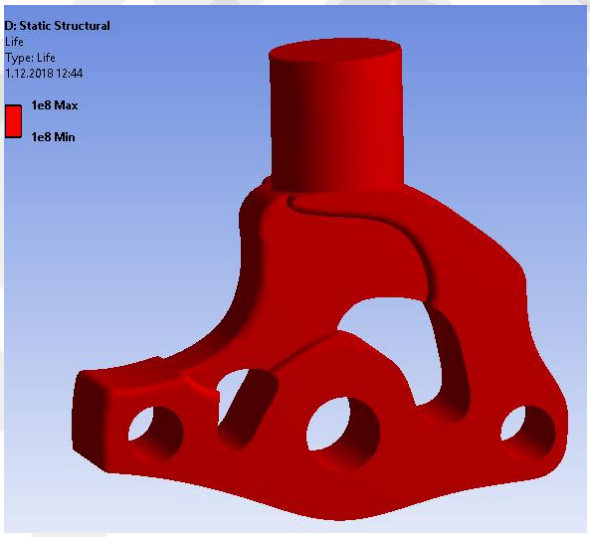

Figure 5.2.1.3 Life analysis result of modified upper side of knee compartment

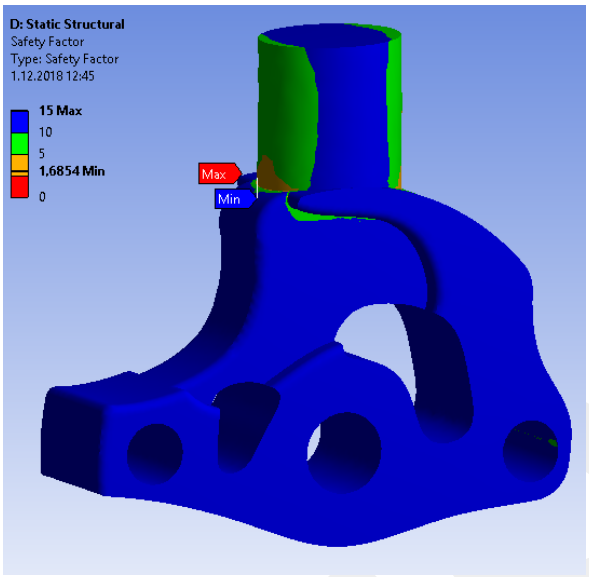

Figure 5.2.1.4 Safety factor result of modified upper side of knee compartment

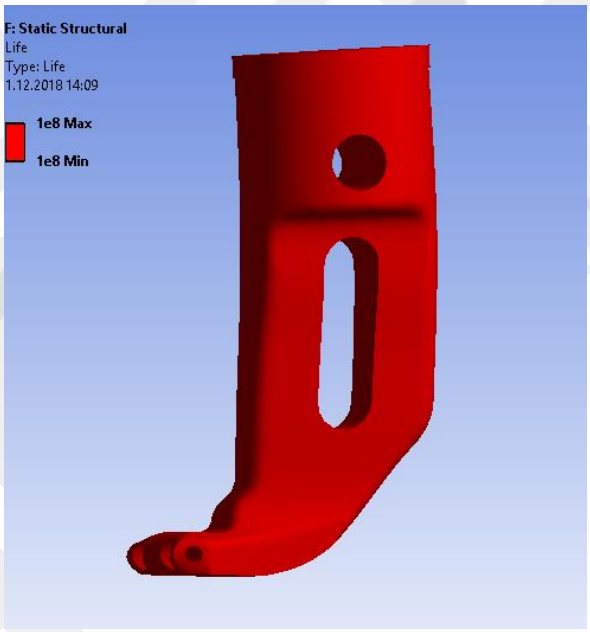

Figure 5.2.1.5 Life analysis result of modified lower part of shank compartment

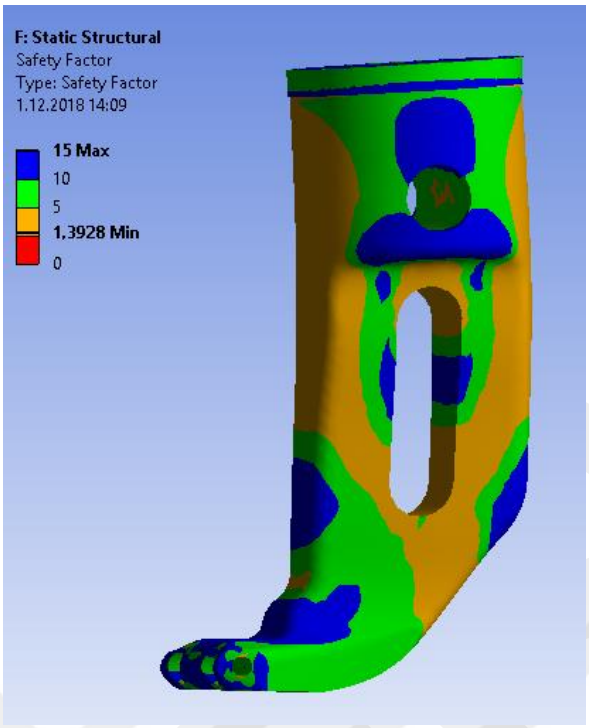

Figure 5.2.1.6 Safety factor result of modified lower part of shank compartment

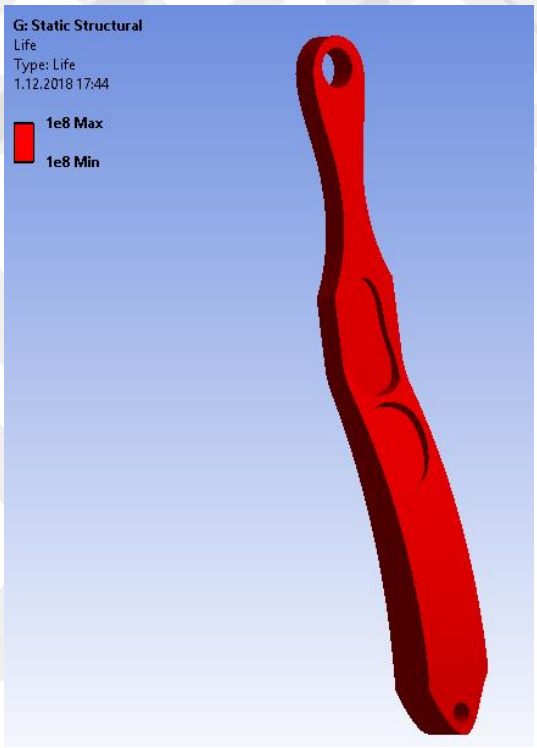

Figure 5.2.1.7 Life analysis of the modified connection part.

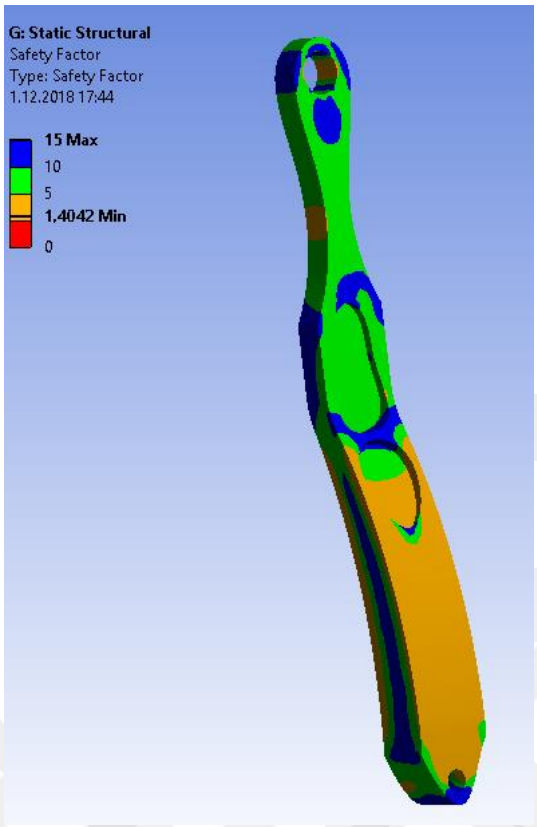

Figure 5.2.1.8 Safety factor of the modified connection part

According to safety factor and life analyses in Ansys, it is clear that parts are in safe side. And the lives of parts are acceptable. Still according to safety factor figures, some areas of parts are seemed to be over safe. But after topology optimization result is exported, the part is not producible, so in terms of producing the part with the help of standard machining methods, the raw result needs to be modified in CAD environment so, after the part is modified, the safety factor is increased consequently. Also, for connection part, initially the part wasn't safe to be used, and it was modified and after that the part was optimized by using topology optimization process. In Table 5.2.1.1 initial model's properties were given.

Moreover, initial weights of parts and modified weights of parts are shown in Table 5.2.1.1.

Initial Design	Optimized Part	Percent of Decreased Weight and Volume
 1.181 kg 420 cm^3	 0,145 kg 51 cm^3	%87,7
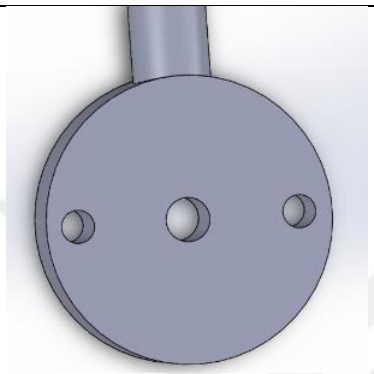 1.335 kg 475 cm^3	 0,600 kg 213 cm^3	%55
 0,327 kg 116 cm^3	 0,164 kg 58 cm^3	%49,8

		%21,6
0,288 kg 102,6 cm^3	0,226 kg 80,4 cm^3	

Table 5.2.1.1 Optimization results in terms of mass reduction

In this chapter totally four parts of prosthesis were optimized and totally weight of prosthesis decreased as 1996 kg and volume of the prosthesis was decreased as 711,2 cm^3. Modified conceptual prosthesis is shown in Figure 5.2.1.9.

Figure 5.2.1.9 Assembly of the partially optimized prosthesis

Chapter 6

Conclusions and Future Prospects

6.1 Conclusions

In this study, a conceptual prosthesis for weight acceptance, stair ascending and sit–to-stand motions are presented. Firstly, the literature was studied and in literature, as underlined in introduction chapter, it is clear that transfemoral prostheses draw attention in last decades. And again as underlined in the introduction chapter, it is possible to make a passive transfemoral prosthesis for walking [44,45]. However for other activities like stair climbing, active parts needs to be implemented to design [46,47]. So, designing a semi-active prosthesis was decided.

In design phase of the study firstly human biomechanical data sets were analyzed and according to these data sets, initial conceptual design of the prosthesis was formed and described in chapter 3. The prosthesis was designed for 80 kg and 1.80m individual. As underlined in chapter 3, initial prototype of the conceptual design was built by using 3D printer as well. By taking into account 3D printed model, problems on the design was examined. Firstly, parts which are at the back side of prosthesis could be problematic. Because while sitting they could block the motion. So, the parts were needed to be modified. Actually, this was the basic reason of modifying the prosthesis in chapter 4.

In chapter 4, modified prosthesis is presented. In this chapter, modified parts are highlighted and also coefficients of elastic elements that are used for motions are

described. To be able to do this, human data sets were analyzed. And according to graphics of natural data and simulated design data it is observed that the new conceptual design nearly mimics the behavior of joints. And also used elastic element for stair ascending decreases the needed power from the actuator by releasing the stored energy during first 40% of cycle by 100W. Still the parts were heavy and the prosthesis should be light. So, for this purpose parts needed to be optimized. The chapter 5 is based on this necessity.

In chapter 5, optimization of the foot-ankle compartments, upper side of the knee, lower part of the shank and connection parts are described. Before these optimization processes the knee design was changed partly to make it light and compact without changing the dimensions and distances of joint in design. And after that, in Ansys environment the parts were optimized and according to resulting shapes, new parts were designed which can be produced by using conventional machining methods. At the end of the optimization process, the weight of parts which were optimized, were decreased as 1,996 kg and also volume of the parts were decreased as 711,2 cm^3. Totally weight and volume of the optimized parts were decreased as 63,7%.

6.2 Future Prospects

In this study, the new semi-active conceptual design for walking with weight acceptance, sit-to-stance and stair climbing is presented and called as WalkMECH V2. The prosthesis was studied in terms of working principle, elastic elements, their coefficient and their behaviors in motions and also structural analyses of parts and their optimizations were depicted in this study.

It is clear that prostheses are composed of many parts so, there are lots of parts to be studied on in terms of functionality and stability. The most critical parts in design were optimized as depicted in chapter 5 but still there are many other parts on the prosthesis that needs to be optimized to make the prosthesis as light as possible. Because of that, the design is currently in initial conceptual stage.

Also, the initial prototype of the prosthesis is currently being built by using CNC machining methods as it is shown in Figure 6.2.1. Moreover, in this prototype, an elastic element which will make the angle of ankle after toe off 0° will be added according to final assembled weight of the foot compartment of the prosthesis.

The parts can be tested for fatigue behavior to validate the FEM results. Moreover, this prototype would be useful to examine the design and testing mechanisms. After stability, functioning and weight of the prosthesis are ensured, the prosthesis needs to be revised according to results and needs to be tested on subjects and validated with these experiments in terms of functionality and biomechanical performance.

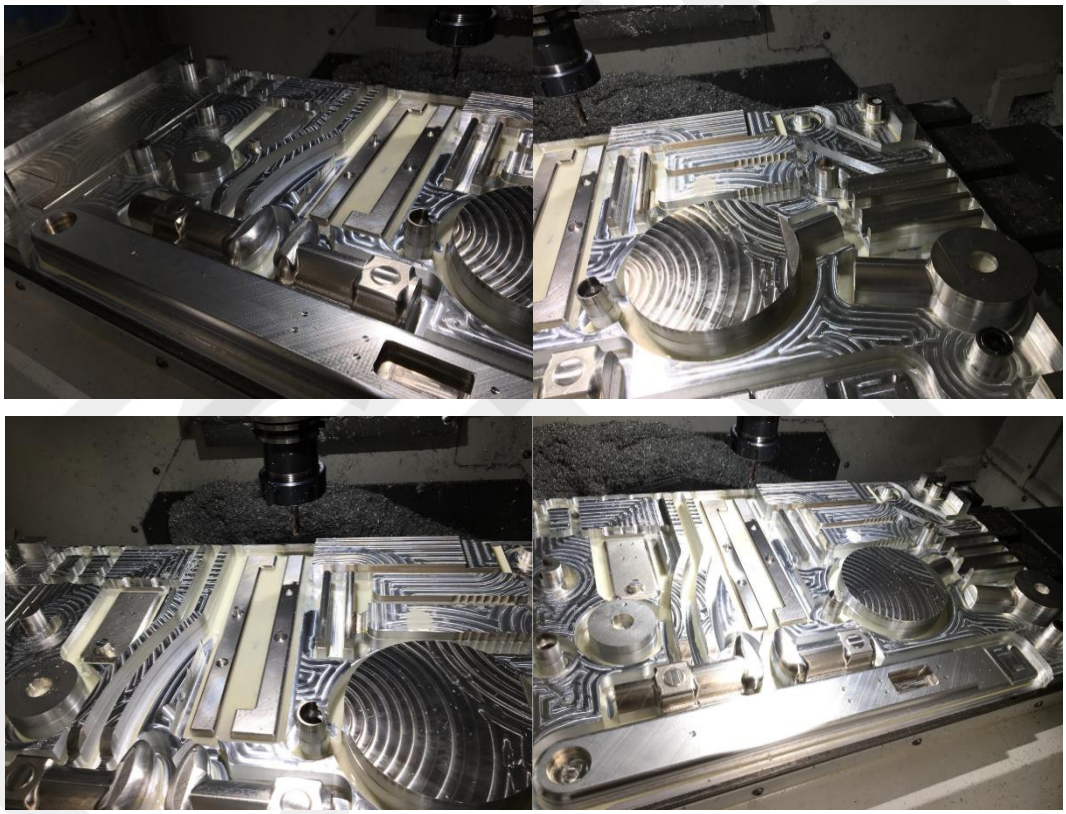

Figure 6.2.1 Production of the initial prototype of the conceptual prosthesis

BIBLIOGRAPHY

[1] NHSScotland, "The Amputee Statistical Database for the UK: 2004/05 Report," *ISD Publ.*, pp. 1–48, 2005.

[2] C. Todor-Locke and D. R. Bassett Jr, "How many steps per day are enough?," *Sport. Med.*, vol. 34, no. February 2004, pp. 1–8, 2004.

[3] R. E. Cowan, B. J. Fregly, M. L. Boninger, L. Chan, M. M. Rodgers, and D. J. Reinkensmeyer, "Recent trends in assistive technology for mobility," *J. Neuroeng. Rehabil.*, vol. 9, no. 1, pp. 1–8, 2012.

[4] M. R. Tomita, W. C. Mann, L. F. Fraas, and K. M. Stanton, "Predictors of the Use of Assistive Devices That Address Physical Impairments among Community-Based Frail Elders," *J. Appl. Gerontol.*, vol. 23, no. 2, pp. 141–155, 2004.

[5] M. Arnout, C. Pierre, V. D. Michael, V. Bram, and L. Dirk, "Concept and design of the HEKTA (Harvest Energy from the Knee and Transfer it to the Ankle) transfemoral prosthesis," *Proc. IEEE RAS EMBS Int. Conf. Biomed. Robot. Biomechatronics*, pp. 550–555, 2012.

[6] T. K. Wang, M. S. Ju, and Y. G. Tsuei, "Adaptive Control of Above Knee Electro-Hydraulic Prosthesis," *J. Biomech. Eng.*, vol. 114, no. August, pp. 421–424, 1992.

[7] H. A. Varol, F. Sup, and M. Goldfarb, "Powered sit-to-stand and assistive stand-to-sit framework for a powered transfemoral prosthesis," *2009 IEEE Int. Conf. Rehabil. Robot. ICORR 2009*, pp. 645–651, 2009.

[8] M. Marino *et al.*, "Access to prosthetic devices in developing countries: Pathways and challenges," *Proc. 5th IEEE Glob. Humanit. Technol. Conf. GHTC 2015*, pp. 45–51, 2015.

[9] M. F. Owings and L. J. Kozak, "Ambulatory and inpatient procedures in the United States, 1996.," *Vital Health Stat. 13.*, no. 139, pp. 1–119, 1998.

[10] World Health Organisation (WHO) and International Society for Prosthetics and Orthotics (ISPO), "Guidelines for training Personnel in Developing countries for Prosthetics and Orthotics Services," *WHO Libr. Cat. Data*, pp. 1–57, 2005.

[11] "WHO standards for prosthetics and orthotics," *Geneva World Heal. Organ. 2017*, 2017.

[12] M. V. Pillai, H. Kazerooni, and A. Hurwich, “Design of a semi-active knee-ankle prosthesis,” *Proc. - IEEE Int. Conf. Robot. Autom.*, pp. 5293–5300, 2011.

[13] B. G. A. Lambrecht and H. Kazerooni, “Design of a semi-active knee prosthesis,” *Proc. - IEEE Int. Conf. Robot. Autom.*, pp. 639–645, 2009.

[14] R. Jiménez-Fabián and O. Verlinden, “Review of control algorithms for robotic ankle systems in lower-limb orthoses, prostheses, and exoskeletons,” *Med. Eng. Phys.*, vol. 34, no. 4, pp. 397–408, 2012.

[15] J.-H. Kim and J.-H. Oh, “Development of an above knee prosthesis using MR damper and leg simulator,” *Proc. 2001 ICRA. IEEE Int. Conf. Robot. Autom.*, vol. 4, pp. 3686–3691, 2001.

[16] M. J. Khan, M. R. Afzal, N. Naseer, and Z. U. Koreshi, “Control system design for a prosthetic leg using series damping actuator,” *2012 Int. Conf. Robot. Artif. Intell. ICRAI 2012*, pp. 1–6, 2012.

[17] R. L. Waters, J. Perry, D. Antonelli, and H. Hislop, “Energy cost of walking of amputees : the influence of level of amputation,” *J. Bone Jt. Surg.*, pp. 42–46, 1976.

[18] D. A. Winter, *“The biomechanics and motor control of human gait : normal, elderly and pathological.”* University of Waterloo Press, 1991.

[19] F. Sup, A. Bohara, and M. Goldfarb, “Design and control of a powered transfemoral prosthesis,” *Int. J. Rob. Res.*, vol. 27, no. 2, pp. 263–273, 2008.

[20] A. H. Shultz, B. E. Lawson, and M. Goldfarb, “Running with a powered knee and ankle prosthesis,” *IEEE Trans. Neural Syst. Rehabil. Eng.*, vol. 23, no. 3, pp. 403–412, 2015.

[21] D. B. Popović and T. Sinkjær, Eds., *“Control of Movement for the Physically Disabled.”* London: Springer London, 2000.

[22] A. O. Kapti and M. S. Yucenur, “Design and control of an active artificial knee joint,” *Mech. Mach. Theory*, vol. 41, no. 12, pp. 1477–1485, 2006.

[23] B. Lawson, H. A. Varol, A. Huff, E. Erdemir, and M. Goldfarb, “Control of Stair Ascent and Descent With a Powered Transfemoral Prosthesis,” *IEEE Trans. Neural Syst. Rehabil. Eng.*, vol. 21, no. 3, pp. 466–473, May 2013.

[24] R. Dedić and H. Dindo, “SmartLeg: An intelligent active robotic prosthesis for lower-limb amputees,” *2011 23rd Int. Symp. Information, Commun. Autom. Technol. ICAT 2011*, 2011.

[25] R. Versluys *et al.*, “A pneumatically powered below-knee prosthesis: Design specifications and first experiments with an amputee,” *Proc. 2nd Bienn. IEEE/RAS-EMBS Int. Conf. Biomed. Robot. Biomechatronics, BioRob 2008*, pp. 372–377, 2008.

[26] A. M. Dollar and H. Herr, “Lower Extremity Exoskeletons and Active Orthoses:Challenges and State-of-the-Art,” *IEEE Trans. Robot.*, vol. 24, no. 1, pp. 144–158, 2008.

[27] Z. W. Lui, M. I. Awad, A. Abouhossein, A. A. Dehghani-Sanij, and N. Messenger, “Virtual prototyping of a semi-active transfemoral prosthetic leg,” *Proc. Inst. Mech. Eng. Part H J. Eng. Med.*, vol. 229, no. 5, pp. 350–361, 2015.

[28] J. K. Hitt, T. G. Sugar, M. Holgate, and R. Bellman, “An Active Foot-Ankle Prosthesis With Biomechanical Energy Regeneration,” *J. Med. Device.*, vol. 4, no. 1, p. 011003, 2010.

[29] A. J. van den Bogert, S. Samorezov, B. L. Davis, and W. A. Smith, “Modeling and Optimal Control of an Energy-Storing Prosthetic Knee,” *J. Biomech. Eng.*, vol. 134, no. 5, p. 051007, 2012.

[30] F. Rohani, H. Richter, and A. J. Van Den Bogert, “Optimal design and control of an electromechanical transfemoral prosthesis with energy regeneration,” *PLoS One*, vol. 12, no. 11, pp. 1–13, 2017.

[31] T. B. Rick Rarick, Hanz Richter, Antonie van den Bogert, Dan Simon, Holly Warner, “Optimal Design of a Transfemoral Prosthesis with Energy Storage and Regeneration,” in *PLoS ONE*, 2014, vol. 12, no. 11, pp. 4108–4113.

[32] H. . Bayram, “Recent Developments in Above-Knee Prosthetics and the Importance of Energy Recovery in Transfemoral Amputee Gait,” *Phys. Med. Rehabil. / Fiz. Tıp ve Rehabil.*, vol. 6, no. 2, pp. 61–68, 2015.

[33] R. D. Bellman, M. A. Holgate, and T. G. Sugar, “SPARKy 3 : Design of an Active Robotic Ankle Prosthesis with Two Actuated Degrees of Freedom Using Regenerative Kinetics .,” pp. 511–516, 2008.

[34] Glabiszewski, “Articulate Joint For Prosthetic Devices,” U.S. Patent, 3863274, 1975.

[35] “3R80 knee joint | Ottobock TR.” [Online]. Available: https://www.ottobock.com.tr/tr/protezler/products-from-a-to-z/knee-joint-3r80/. [Accessed: 14-Nov-2018].

[36] “C LEG | Ottobock TR.” [Online]. Available: https://www.ottobock.com.tr/tr/protezler/lower-limb/solution-overview/knee-joint-c-leg/. [Accessed: 14-Nov-2018].

[37] “RHEO KNEE.” [Online]. Available: https://www.ossur.com/prosthetic-solutions/products/dynamic-solutions/rheo-knee. [Accessed: 14-Nov-2018].

[38] Bedard, “Actuated Leg Prosthesis For Above-Knee Amputees,” U.S. Patent, 7314490, 2008.

[39] R. Ünal, S. M. Behrens, R. Carloni, E. E. G. Hekman, S. Stramigioli, and H. F. J.

M. Koopman, “A Prosthetic or Ortothic Device and a Method for Using Such a Device,” Patent PCT/NL2012/050421, 2012.

[40] R. Unal, R. Carloni, E. E. G. Hekman, S. Stramigioli, and H. F. J. M. Koopman, “Conceptual design of an energy efficient transfemoral prosthesis,” in *IEEE/RSJ 2010 International Conference on Intelligent Robots and Systems, IROS 2010 - Conference Proceedings*, 2010, pp. 343–348.

[41] R. Unal, S. M. Behrens, R. Carloni, E. E. G. Hekman, S. Stramigioli, and H. F. J. M. Koopman, “Prototype design and realization of an innovative energy efficient transfemoral prosthesis,” in *2010 3rd IEEE RAS & EMBS International Conference on Biomedical Robotics and Biomechatronics*, 2010, pp. 191–196.

[42] R. Unal, R. Carloni, S. M. Behrens, E. E. G. Hekman, S. Stramigioli, and H. F. J. M. Koopman, “Towards fully passive energy efficient transfemoral prosthesis,” in *IEEE/RAS-EMBS International Conference on Biomedical Robotics and Biomechatronics (BioRob)*, 2012.

[43] R. Unal *et al.*, “The control of recycling energy strorage capacity for WalkMECHadapt,” in *The 23rd IEEE International Symposium on Robot and Human Interactive Communication*, 2014, pp. 720–725.

[44] D. A. Winter, “Energy Generation and Absorption at the Ankle and Knee during Fast, Natural, and Slow Cadences,” *Clin. Orthop. Relat. Res.*, no. 175, pp. 147–154, 1983.

[45] D. A. Winter, “Biomechanical motor patterns in normal walking,” *J. Mot. Behav.*, vol. 15, no. 4, pp. 302–330, 1983.

[46] H. Argunsah Bayram, C.-H. Chien, and B. L. Davis, “Active functional stiffness of the knee joint during activities of daily living: A parameter for improved design of prosthetic limbs,” *Clin. Biomech.*, vol. 29, no. 10, pp. 1193–1199, Dec. 2014.

[47] R. Riener, M. Rabuffetti, and C. Frigo, “Joint powers in stair climbing at different slopes,” in *Proceedings of the First Joint BMES/EMBS Conference. 1999 IEEE Engineering in Medicine and Biology 21st Annual Conference and the 1999 Annual Fall Meeting of the Biomedical Engineering Society (Cat. No.99CH37015)*, vol. 1, p. 530.

[48] R. Unal *et al.*, “Modeling of WalkMECH: A fully-passive energy-efficient transfemoral prosthesis prototype,” *IEEE Int. Conf. Rehabil. Robot.*, 2013.

[49] L. C. Vaughan, L. B. Davis, and J. O’Conner, *“Dynamics of Human Gait,”* 2nd ed. Kiboho Publishers, 1992.

[50] J. Perry, “Gait Analysis: Normal and Pathological Function.,” *SLACK Inc.*, 1992.

[51] Streifender, “The eight phases of human gait cycle.” [Online]. Available: https://www.streifeneder.com/downloads/o.p./400w43_e_poster_gangphasen_druck.pdf. [Accessed: 10-Dec-2018].

[52] D. A. Winter, *"The biomechanics and motor control of human gait."* 1987.

[53] R. Riener, M. Rabuffetti, and C. Frigo, "Stair ascent and descent at different inclinations," *Gait Posture*, vol. 15, no. 1, pp. 32–44, 2002.

[54] R. F. Muraca and J. S. Whittick, *"Materials Hand Book Aluminium Alloy 7075 (2nd edition)."* United States, 1972.

[55] F. Sup, A. Bohara, and M. Goldfarb, "Design and Control of a Powered Transfemoral Prosthesis," *Int. J. Rob. Res.*, vol. 27, no. 2, pp. 263–273, Feb. 2008.

[56] M. P. Bendsøe and O. Sigmund, *"Topology optimization : theory, methods, and applications."* Springer, 2003.

[57] N. Jain, R. Joshi, and R. Saxena, "Topological Optimization Techniques For Linear Isotropic Structures Subjected TO Static And Self-Weight Loading Conditions," *Int. Res. J. Eng. Technol.*, 2015.

[58] P. Kohnke, *"Theory Reference for the Mechanical APDL and Mechanical Applications,"* no. April. 2009.

[59] A. W. Gebisa and H. G. Lemu, "A case study on topology optimized design for additive manufacturing," *IOP Conf. Ser. Mater. Sci. Eng.*, vol. 276, no. 1, 2017.

[60] ANSYS, "ANSYS 13.0 Meshing User's Guide," *Knowl. Creat. Diffus. Util.*, no. November, 2010.

[61] "Aluminum 7075-T6; 7075-T651." [Online]. Available: http://www.matweb.com/search/DataSheet.aspx?MatGUID=4f19a42be94546b686bbf43f79c51b7d&ckck=1. [Accessed: 16-Nov-2018].